clinical efficacy, a computed tomography (CT) scan was performed a few days before enrollment and also after the treatment. In some cases with partial responses, we observed that the enhanced area decreased in size, and necrosis appeared at the center of the tumor.

These encouraging clinical studies on advance lung cancers and head and neck tumors warrant further evaluation of NKT cell-targeted immunotherapy for survival benefit. In general, the immunotherapy may be more effective in patients with low tumor burden. Currently, we have been conducting α-GalCer/DC therapy for stage IIA to IIIA lung cancer patients with small tumor foci, including remaining micro-metastasis after radical surgery or after receiving the established first-line therapy in collaboration with National Hospital Organization.

FUTURE DIRECTIONS FOR NKT CELL-MEDIATED CANCER THERAPY USING iPS-DERIVED NKT CELLS

Although an NKT cell-targeted therapy has been shown to have significant clinical efficacy, only one third of patients are eligible in the case of advanced non-small lung cancer patients; the frequency of NKT cells in the other patients is too low. To overcome this problem, we established *in vitro* methods for generation of unlimited numbers of functional NKT cells, which then can be transferred into the patients whose endogenous NKT cell numbers are limited.

Induced pluripotent stem (iPS) cells were generated from mature NKT cells using *Oct3/4*, *Sox2*, *Klf4*, and *c-Myc* genes and then were developed into functional NKT cells *in vitro* in the presence of IL-7 and Flt3L according to the conventional protocol (42–44). The NKT cells generated *in vitro* from iPS-NKT cells were functional in the *in vivo* setting using the experimental model of OVA as an artificial tumor antigen (44). When NKT-KO mice were reconstituted with iPS-derived NKT cells followed by immunization with OVA and α-GalCer, we detected a 70-fold increase in the number of OVA-specific IFN-γ producing $CD8^+$ T cells above that seen in the control mice (**Figure 2A**). Under these conditions, the growth of the OVA-expressing EL4 (EG7) tumor cells was suppressed (**Figure 2B**). Thus, the iPS-derived NKT cells are able to function *in vivo*.

Before any clinical application of iPS-derived NKT cells, two immunological issues need to be addressed, one is whether GvHD is induced by NKT cells and the other is whether semi-allogeneic NKT cells will work *in vivo*, because of the clinical use of iPS-derived NKT cells under semi-allogeneic conditions. To address the first question, iPS-derived NKT cells on a B6 background and B6 or BALB/c CD4 T cells were injected into BALB/c RAG-KO mice. The results were very clear: only B6 CD4T cells, but not iPS-derived B6 NKT cells or BALB/c CD4 T cells, induced GvHD characterized by weight loss, diarrhea, skin disease development, or death after cell transfer. Concerning the second issue of the functional potential of semi-allogeneic NKT cells *in vivo* (129xB6) F1 NKT cells derived from cloned ES cells established by nuclear transfer of mature NKT cells into unfertilized eggs were injected into B6 NKT-KO mice and analyzed for their adjuvant activity in the OVA model. Significant proliferation of OVA-specific CD8 killer T cells was detected, even though these cells are eliminated in a few days. The ability to generate NKT cells using a simple *in vitro* culture system offers a powerful approach for the establishment of optimal NKT cell therapy. Our clinical application of the iPS-derived NKT cell therapy program has now been selected as a Center for Clinical Application Research on Specific Disease/Organ (Type B) in the Research Center Network for Realization of Regenerative Medicine, Japan.

FUTURE DIRECTIONS FOR THE NEXT GENERATION OF NKT CELL-TARGETED THERAPY

For the establishment of the next generation of NKT cell-targeted therapy, we developed artificial adjuvant vector cells to induce both innate and long-term memory CD8T cell responses against cancer. In this system, allogeneic NIH3T3 fibroblasts were used as a vector cell, into which tumor antigen mRNA and CD1d with α-GalCer were introduced. In the model experiment, we used OVA mRNA as an artificial tumor antigen together with α-GalCer/CD1d to induce the NKT cell-mediated adjuvant effects *in vivo in situ* (**Figure 2C**) (22). The allogeneic artificial vector cells were destroyed by the host immune system soon after inoculation and all materials carried by the cells were taken up by the host DCs, which immediately stimulated host NKT cells followed by induction of DC maturation and also by activation of innate NK cells and adaptive OVA-specific CD8 killer T cells. Surprisingly, long-term memory CD8 T cell responses were induced in an antigen-specific manner and persisted even 1 year after the initial single injection and suppressed OVA-expressing tumor cell metastasis (**Figures 2D,E**) (45). To test if this method could be generalized, we used TRP-2, tyrosinase related protein-2, which is a weak tumor antigen expressed by both mouse and human melanoma cells as the tumor antigen, and successfully suppressed tumor growth *in vivo*. Therefore, the artificial vector cells should be useful in the future for vaccines against various tumors.

SUMMARY

Natural killer T cells bridge innate and adaptive immunity, which enhances protective immune responses and also establishes long-term memory responses. Therefore, NKT cells have important therapeutic potential. In support of this notion, clinical trials on NKT cell-targeted therapy have demonstrated clinical safety and significant clinical efficacy in terms of prolonged median overall survival time in lung cancer patients and achieved stable disease status or partial responses in head or neck cancer patients.

The powerful treatment options for the future are to establish iPS cells that can generate unlimited numbers of NKT cells with adjuvant activity *in vitro* and suppress tumor growth *in vivo*. The other option is to establish the artificial adjuvant vector cells containing tumor mRNA and α-GalCer/CD1d, which have been shown to induce tumor-specific long-term memory CD8T cell responses and to inhibit tumor growth even 1 year after single injection. Thus, these could be therapeutic candidates for the next generation of NKT cell-targeted therapy.

REFERENCES

1. Taniguchi M, Harada M, Kojo S, Nakayama T, Wakao H. The regulatory role of Vα14 NKT cells in innate and acquired immune response. *Annu Rev Immunol* (2003) **21**:483–513. doi:10.1146/annurev.immunol.21.120601.141057

2. Godfrey DI, MacDonald HR, Kronenberg M, Smyth MJ, Van Kaer L. NKT cells: what's in a name? *Nat Rev Immunol* (2004) **4**(3):231–7. doi:10.1038/nri1309
3. Bendelac A, Savage PB, Teyton L. The biology of NKT cells. *Annu Rev Immunol* (2007) **25**:297–336. doi:10.1146/annurev.immunol.25.022106.141711
4. Imai K, Kanno M, Kimoto H, Shigemoto K, Yamamoto S, Taniguchi M. Sequence and expression of transcripts of the T-cell antigen receptor alpha-chain gene in a functional, antigen-specific suppressor-T-cell hybridoma. *Proc Natl Acad Sci U S A* (1986) **83**(22):8708–12. doi:10.1073/pnas.83.22.8708
5. Koseki H, Imai K, Ichikawa T, Hayata I, Taniguchi M. Predominant use of a particular alpha-chain in suppressor T cell hybridomas specific for keyhole limpet hemocyanin. *Int Immunol* (1989) **1**(6):557–64. doi:10.1093/intimm/1.6.557
6. Koseki H, Imai K, Nakayama F, Sado T, Moriwaki K, Taniguchi M. Homogenous junctional sequence of the V14+ T-cell antigen receptor alpha chain expanded in unprimed mice. *Proc Natl Acad Sci U S A* (1990) **87**(14):5248–52. doi:10.1073/pnas.87.14.5248
7. Cui J, Shin T, Kawano T, Sato H, Kondo E, Toura I, et al. Requirement for V<συβ>α</συβ>14 NKT cells in IL-12-mediated rejection of tumors. *Science* (1997) **278**:1623–6. doi:10.1126/science.278.5343.1623
8. Adachi Y, Koseki H, Zijlstra M, Taniguchi M. Positive selection of invariant V alpha 14+ T cells by non-major histocompatibility complex-encoded class I-like molecules expressed on bone marrow-derived cells. *Proc Natl Acad Sci U S A* (1995) **92**(4):1200–4. doi:10.1073/pnas.92.4.1200
9. Zeng Z, Castano AR, Segelke BW, Stura EA, Peterson PA, Wilson IA. Crystal structure of mouse CD1: an MHC-like fold with a large hydrophobic binding groove. *Science* (1997) **277**(5324):339–45. doi:10.1126/science.277.5324.339
10. Kawano T, Cui J, Koezuka Y, Toura I, Kaneko Y, Motoki K, et al. CD1d-restricted and TCR-mediated activation of Vα14 NKT cells by glycosylceramides. *Science* (1997) **278**:1626–9. doi:10.1126/science.278.5343.1626
11. Kawano T, Tanaka Y, Shimizu E, Kaneko Y, Kamata N, Sato H, et al. A novel recognition motif of human NKT antigen receptor for a glycolipid ligand. *Int Immunol* (1999) **11**(6):881–7. doi:10.1093/intimm/11.6.881
12. Borg NA, Wun KS, Kjer-Nielsen L, Wilce MC, Pellicci DG, Koh R, et al. CD1d-lipid-antigen recognition by the semi-invariant NKT T-cell receptor. *Nature* (2007) **448**(7149):44–9. doi:10.1038/nature05907
13. Spada FM, Koezuka Y, Porcelli SA. CD1d-restricted recognition of synthetic glycolipid antigens by human natural killer T cells. *J Exp Med* (1998) **188**:1529–34. doi:10.1084/jem.188.8.1529
14. Brossay L, Chioda M, Burdin N, Koezuka Y, Casorati G, Dellabona P, et al. CD1d-mediated recognition of an α-galactosylceramide by natural killer T Cells is highly conserved through mammalian evolution. *J Exp Med* (1998) **188**:1521–8. doi:10.1084/jem.188.8.1521
15. Brigl M, Brenner MB. CD1: antigen presentation and T cell function. *Annu Rev Immunol* (2004) **22**:817–90. doi:10.1146/annurev.immunol.22.012703.104608
16. Taniguchi M, Seino K, Nakayama T. The NKT cell system: bridging innate and acquired immunity. *Nat Immunol* (2003) **4**(12):1164–5. doi:10.1038/ni1203-1164
17. Fujii S, Shimizu K, Smith C, Bonifaz L, Steinman RM. Activation of natural killer T cells by α-galactosylceramide rapidly induces the full maturation of dendritic cells in vivo and thereby acts as an adjuvant for combined CD4 and CD8 T cell immunity to a co-administered protein. *J Exp Med* (2003) **198**(2):267–79. doi:10.1084/jem.20030324
18. Hermans IF, Silk JD, Gileadi U, Salio M, Mathew B, Ritter G, et al. NKT cells enhance $CD4^+$ and $CD8^+$ T cell responses to soluble antigen in vivo through direct interaction with dendritic cells. *J Immunol* (2003) **171**:5140–7.
19. Eberl G, Brawand P, MacDonald HR. Selective bystander proliferation of memory CD4+ and CD8+ T cells upon NK T or T cell activation. *J Immunol* (2000) **165**(8):4305–11.
20. Gumperz JE, Roy C, Makowska A, Lum D, Sugita M, Podrebarac T, et al. Murine CD1d-restricted T cell recognition of cellular lipids. *Immunity* (2000) **12**:211–21. doi:10.1016/S1074-7613(00)80174-0
21. Pardoll DM. The blockade of immune checkpoints in cancer immunotherapy. *Nat Rev Cancer* (2012) **12**(4):252–64. doi:10.1038/nrc3239
22. Fujii S, Goto A, Shimizu K. Antigen mRNA-transfected, allogeneic fibroblasts loaded with NKT-cell ligand confer antitumor immunity. *Blood* (2009) **113**(18):4262–72. doi:10.1182/blood-2008-08-176446
23. Lippitz BE. Cytokine patterns in patients with cancer: a systematic review. *Lancet Oncol* (2013) **14**(6):e218–28. doi:10.1016/S1470-2045(12)70582-X
24. Fujii S, Liu K, Smith C, Bonito AJ, Steinman RM. The linkage of innate to adaptive immunity via maturing dendritic cells in vivo requires CD40 ligation in addition to antigen presentation and CD80/86 costimulation. *J Exp Med* (2004) **199**(12):1607–18. doi:10.1084/jem.20040317
25. Akutsu Y, Nakayama T, Harada M, Kawano T, Motohashi S, Shimizu E, et al. Expansion of lung V alpha 14 NKT cells by administration of alpha-galactosylceramide-pulsed dendritic cells. *Jpn J Cancer Res* (2002) **93**(4):397–403. doi:10.1111/j.1349-7006.2002.tb01270.x
26. Motohashi S, Kobayashi S, Ito T, Magara KK, Mikuni O, Kamada N, et al. Preserved IFN-γ production of circulating Vα24 NKT cells in primary lung cancer patients. *Int J Cancer* (2002) **102**(2):159–65. doi:10.1002/ijc.10678
27. Toura I, Kawano T, Akutsu Y, Nakayama T, Ochiai T, Taniguchi M. Inhibition of experimental tumor metastasis by dendritic cells pulsed with α-galactosylceramide. *J Immunol* (1999) **163**:2387–91.
28. Motohashi S, Nagato K, Kunii N, Yamamoto H, Yamasaki K, Okita K, et al. A phase I-II study of α-galactosylceramide-pulsed IL-2/GM-CSF-cultured peripheral blood mononuclear cells in patients with advanced and recurrent non-small cell lung cancer. *J Immunol* (2009) **182**(4):2492–501. doi:10.4049/jimmunol.0800126
29. Ishikawa E, Motohashi S, Ishikawa A, Ito T, Uchida T, Kaneko T, et al. Dendritic cell maturation by CD11c- T cells and Valpha24+ natural killer T-cell activation by alpha-galactosylceramide. *Int J Cancer* (2005) **117**(2):265–73. doi:10.1002/ijc.21197
30. Ishikawa A, Motohashi S, Ishikawa E, Fuchida H, Higashino K, Otsuji M, et al. A phase I study of α-galactosylceramide (KRN7000)-pulsed dendritic cells in patients with advanced and recurrent non-small cell lung cancer. *Clin Cancer Res* (2005) **11**(5):1910–7. doi:10.1158/1078-0432.CCR-04-1453
31. Motohashi S, Ishikawa A, Ishikawa E, Otsuji M, Iizasa T, Hanaoka H, et al. A phase I study of in vitro expanded natural killer T cells in patients with advanced and recurrent non-small cell lung cancer. *Clin Cancer Res* (2006) **12**(20 Pt 1):6079–86. doi:10.1158/1078-0432.CCR-06-0114
32. Motohashi S, Okamoto Y, Yoshino I, Nakayama T. Anti-tumor immune responses induced by iNKT cell-based immunotherapy for lung cancer and head and neck cancer. *Clin Immunol* (2011) **140**(2):167–76. doi:10.1016/j.clim.2011.01.009
33. Motohashi S, Nakayama T. Clinical applications of natural killer T cell-based immunotherapy for cancer. *Cancer Sci* (2008) **99**(4):638–45. doi:10.1111/j.1349-7006.2008.00730.x
34. Carnaud C, Lee D, Donnars O, Park SH, Beavis A, Koezuka Y, et al. Cutting edge: cross-talk between cells of the innate immune system: NKT cells rapidly activate NK cells. *J Immunol* (1999) **163**(9):4647–50.
35. Smyth MJ, Crowe NY, Pellicci DG, Kyparissoudis K, Kelly JM, Takeda K, et al. Sequential production of interferon-γ by $NK1.1^+$ T cells and natural killer cells is essential for the antimetastatic effect of α-galactosylceramide. *Blood* (2002) **99**:1259–66. doi:10.1182/blood.V99.4.1259
36. Nagato K, Motohashi S, Ishibashi F, Okita K, Yamasaki K, Moriya Y, et al. Accumulation of activated invariant natural killer T cells in the tumor microenvironment after alpha-galactosylceramide-pulsed antigen presenting cells. *J Clin Immunol* (2012) **32**(5):1071–81. doi:10.1007/s10875-012-9697-9
37. Mountain CF. Revisions in the international system for staging lung cancer. *Chest* (1997) **111**(6):1710–7. doi:10.1378/chest.111.6.1710
38. Socinski MA. The role of chemotherapy in the treatment of unresectable stage III and IV nonsmall cell lung cancer. *Respir Care Clin N Am* (2003) **9**(2):207–36. doi:10.1016/S1078-5337(02)00089-8
39. Shepherd FA, Dancey J, Ramlau R, Mattson K, Gralla R, O'Rourke M, et al. Prospective randomized trial of docetaxel versus best supportive care in patients with non-small-cell lung cancer previously treated with platinum-based chemotherapy. *J Clin Oncol* (2000) **18**(10):2095–103.
40. Huisman C, Smit EF, Giaccone G, Postmus PE. Second-line chemotherapy in relapsing or refractory non-small-cell lung cancer: a review. *J Clin Oncol* (2000) **18**(21):3722–30.
41. Yamasaki K, Horiguchi S, Kurosaki M, Kunii N, Nagato K, Hanaoka H, et al. Induction of NKT cell-specific immune responses in cancer tissues after NKT cell-targeted adoptive immunotherapy. *Clin Immunol* (2011) **138**(3):255–65. doi:10.1016/j.clim.2010.11.014
42. Takahashi K, Yamanaka S. Induction of pluripotent stem cells from mouse embryonic and adult fibroblast cultures by defined factors. *Cell* (2006) **126**(4):663–76. doi:10.1016/j.cell.2006.07.024

43. Okita K, Ichisaka T, Yamanaka S. Generation of germline-competent induced pluripotent stem cells. *Nature* (2007) **448**(7151):313–7. doi:10.1038/nature05934
44. Watarai H, Fujii S, Yamada D, Rybouchkin A, Sakata S, Nagata Y, et al. Murine induced pluripotent stem cells can be derived from and differentiate into natural killer T cells. *J Clin Invest* (2010) **120**(7):2610–8. doi:10.1172/JCI42027
45. Shimizu K, Asakura M, Shinga J, Sato Y, Kitahara S, Hoshino K, et al. Invariant NKT cells induce plasmacytoid dendritic cell (DC) cross-talk with conventional DCs for efficient memory CD8+ T cell induction. *J Immunol* (2013) **190**(11):5609–19. doi:10.4049/jimmunol.1300033

Conflict of Interest Statement: The authors declare that the research was conducted in the absence of any commercial or financial relationships that could be construed as a potential conflict of interest.

Received: 06 November 2013; accepted: 11 November 2013; published online: 02 December 2013.
Citation: Fujii S, Shimizu K, Okamoto Y, Kunii N, Nakayama T, Motohashi S and Taniguchi M (2013) NKT cells as an ideal anti-tumor immunotherapeutic. Front. Immunol. 4:409. doi: 10.3389/fimmu.2013.00409
This article was submitted to Tumor Immunity, a section of the journal Frontiers in Immunology.

Gata3/Ruvbl2 complex regulates T helper 2 cell proliferation via repression of Cdkn2c expression

Hiroyuki Hosokawa[a], Tomoaki Tanaka[b,c,d], Miki Kato[a], Kenta Shinoda[a], Hiroyuki Tohyama[a], Asami Hanazawa[a], Yuuki Tamaki[a], Kiyoshi Hirahara[e], Ryoji Yagi[a], Ikue Sakikawa[f], Atsushi Morita[f], Morio Nagira[g], Masha V. Poyurovsky[h], Yutaka Suzuki[i], Shinichiro Motohashi[j], and Toshinori Nakayama[a,d,1]

[a]Department of Immunology, [b]Department of Clinical Cell Biology, and [c]Division of Endocrinology and Metabolism, [e]Department of Advanced Allegology of the Airway, and [j]Department of Medical Immunology, Graduate School of Medicine, Chiba University, 1-8-1 Inohana, Chuo-ku, Chiba 260-8670, Japan; [d]CREST, Japan Science and Technology Agency, 1-8-1 Inohana, Chuo-ku, Chiba 260-8670, Japan; [f]Solution for Medicinal Biology, Innovative Drug Discovery Research Laboratories, [g]Allergy and Oncology, Medicinal Research Laboratories, Shionogi and Co., Ltd., 3-1-1, Futabacho, Toyonaka, Osaka 561-0825, Japan; [h]Molecular Oncology Group, Kadmon Research Institute, New York, NY 10016; and [i]Department of Medical Genome Sciences, Graduate School of Frontier Sciences, University of Tokyo, 5-1-5 Kashiwanoha, Kashiwa, Chiba 277-8562, Japan

Edited by Anjana Rao, La Jolla Institute for Allergy and Immunology, La Jolla, CA, and approved October 10, 2013 (received for review July 3, 2013)

GATA-binding protein 3 (Gata3) controls the differentiation of naive CD4 T cells into T helper 2 (Th2) cells by induction of chromatin remodeling of the Th2 cytokine gene loci, direct transactivation of *Il5* and *Il13* genes, and inhibition of *Ifng*. Gata3 also facilitates Th2 cell proliferation via additional mechanisms that are far less well understood. We herein found that Gata3 associates with RuvB-like protein 2 (Ruvbl2) and represses the expression of a CDK inhibitor, cyclin-dependent kinase inhibitor 2c (*Cdkn2c*) to facilitate the proliferation of Th2 cells. Gata3 directly bound to the *Cdkn2c* locus in an Ruvbl2-dependent manner. The defect in the proliferation of *Gata3*-deficient Th2 cells is rescued by the knockdown of *Cdkn2c*, indicating that Cdkn2c is a key molecule involved in the Gata3-mediated induction of Th2 cell proliferation. Ruvbl2-knockdown Th2 cells showed decreased antigen-induced expansion and caused less airway inflammation in vivo. We therefore have identified a functional Gata3/Ruvbl2 complex that regulates the proliferation of differentiating Th2 cells through the repression of a CDK inhibitor, *Cdkn2c*.

master transcription factor | transcriptional regulation | polycomb group complex

After antigenic stimulation in a particular cytokine milieu, naive CD4 T cells differentiate into various T helper (Th) cell subsets including Th1, Th2, and Th17 cells (1, 2). The differentiation of Th2 cells requires IL-4 stimulation, which leads to Stat6 activation and the induction of GATA-binding protein 3 (*Gata3*) transcription (3, 4). In addition, the Ras-ERK MAPK cascade controls Gata3 stability through the ubiquitin/proteasome-dependent pathway (5, 6). Gata3 is expressed in T lymphocytes, and its expression is required for the CD4 versus CD8 lineage choice and at the β-selection checkpoint in the thymus (7, 8), as well as for Th2 cell differentiation in the periphery (9–12).

It has been known that activated CD4 T cells proliferate more vigorously under the Th2 culture conditions where IL-4 is present compared with the Th1 conditions (13, 14). *Gata3*-deficient Th2 cells show a substantially reduced BrdU incorporation, indicating that Gata3 is involved in the regulation of Th2 cell expansion (15). However, no definitive analysis has yet been reported regarding the molecular mechanisms underlying the Gata3-mediated induction of Th2 cell proliferation.

T-cell proliferation following TCR signaling is stimulated by the increase in the expression levels of CDK4/6 and cyclin D (16). CDK inhibitors including the Ink4 family members *Cdkn2a* (p16, ink4a), *Cdkn2b* (p15, ink4b), *Cdkn2c* (p18, ink4c), and *Cdkn2d* (p19, ink4d) negatively regulate the activity of the cyclin D–CDK4/6 complex and block the G1-S phase transition, halting cellular proliferation in nonimmune cells (17). *Cdkn2c* has been implicated in the regulation of T-cell proliferation, supported by the observation that T cells from *Cdkn2c*-deficient mice exhibit a hyperproliferative phenotype in response to TCR stimulation (18). Although expression of *Cdkn2c* is restrained by GATA3 in mammary luminal progenitor cells, the transcriptional regulation of this gene in Th2 cells is yet to be fully elucidated (19).

We herein identified a Gata3/RuvB-like protein 2 (Ruvbl2) complex as a key regulatory mechanism of Th2 cell proliferation via repression of *Cdkn2c*. Such a regulatory mechanism differs from other cell types and might be uniquely specific for Th2-cell proliferation. Ruvbl2 regulates the recruitment of Gata3 to the *Cdkn2c* locus, and, together, they repress the expression of the *Cdkn2c*. Moreover, the defect in the proliferation of *Gata3*-deficient Th2 cells is rescued by knockdown of *Cdkn2c*, indicating that Cdkn2c is a key molecule involved in the Gata3-mediated induction of Th2 cells. Therefore, the Gata3/Ruvbl2 complex plays a pivotal role in the proliferation of differentiating Th2 cells via the repression of *Cdkn2c*.

Results

Identification of Ruvbl2 as a Molecule That Interacts with Gata3 in Th2 Cells. Gata3 is well-established as a key transcription factor involved in Th2-cell differentiation, but the nature of the functional Gata3 complexes that control the various processes required for Th2-cell generation, including their proliferation, has been unclear. To identity the functional components of the

Significance

GATA-binding protein 3 (Gata3) controls the differentiation of naive CD4 T cells into T helper 2 (Th2) cells by induction of chromatin remodeling at the Th2 cytokine gene loci. Gata3 also facilitates Th2 cell proliferation via unknown mechanisms. We have identified a functional Gata3/RuvB-like protein 2 (Ruvbl2) complex that regulates the proliferation of differentiating Th2 cells through the repression of a CDK inhibitor, cyclin-dependent kinase inhibitor 2c (*Cdkn2c*). Gata3 directly bound to the *Cdkn2c* locus in an Ruvbl2-dependent manner, and Cdkn2c-knockdown experiments indicated an important role for this molecule in the Gata3-mediated induction of Th2-cell proliferation. Ruvbl2-knockdown Th2 cells showed decreased antigen-induced expansion and caused less airway inflammation in vivo, indicating an important role for Ruvbl2 in Th2 cells in allergic reactions.

Author contributions: H.H., T.T., R.Y., S.M., and T.N. designed research; H.H., M.K., K.S., H.T., A.H., Y.T., I.S., A.M., M.N., and Y.S. performed research; H.H., I.S., A.M., M.N., and Y.S. analyzed data; and H.H., T.T., K.H., M.V.P., and T.N. wrote the paper.

The authors declare no conflict of interest.

This article is a PNAS Direct Submission.

Data deposition: The ChIP-seq data have been deposited in the DNA Data Bank of Japan, www.ddbj.nig.ac.jp (accession no. DRA001102).

[1]To whom correspondence should be addressed. E-mail: tnakayama@faculty.chiba-u.jp.

This article contains supporting information online at www.pnas.org/lookup/suppl/doi:10.1073/pnas.1311100110/-/DCSupplemental.

Gata3 complexes, we adopted a unique proteomics approach using affinity purification from the material obtained from the formaldehyde cross-linked Gata3 complex, in which associated molecules with low affinity can be identified (20). The 3xFlag–Gata3 complexes were precipitated efficiently by an anti-Flag mAb from the 3xFlag-tagged Gata3-expressing Th2 cell line, D10G4.1, and a mass-spectrometry analysis identified several polypeptides, including Ruvbl2 (also known as reptin or Tip49b) (Fig. 1*A*). To confirm the association of Gata3 with Ruvbl2, formaldehyde cross-linled cell extracts from the same cells were subjected to immunoprecipitation with an anti-Flag mAb. Ruvbl2 was easily detected in the cross-linked Gata3 complexes, but not in the non–cross-linked Gata3 complexes, thus indicating that there is a low-affinity association of these two molecules in D10G4.1 cells (Fig. 1*B*). The interaction between Gata3 and Ruvbl2 was also detected in non–cross-linked 293T cells in which Flag-tagged Gata3 and Myc-tagged Ruvbl2 were overexpressed (Fig. 1*C*). To address the direct molecular association of these two molecules, a GST–pull-down assay with purified recombinant Gata3 and Ruvbl2 was performed (Fig. 1*D*). The association of Gata3 with Ruvbl2 persisted in the presence of ethidium bromide, suggesting that the association is DNA-independent (Fig. S1). These results indicate that Ruvbl2 is a bona fide Gata3-interacting molecule in Th2 cells.

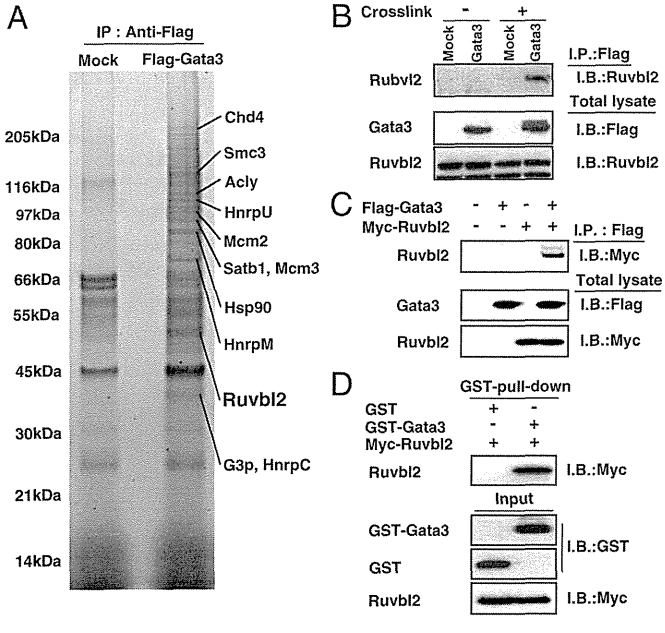

Fig. 1. Identification of Ruvbl2 as a molecule that interacts with Gata3 in Th2 cells. (*A*) Total extracts from 3xFlag–Gata3-expressing cross-linked D10G4.1 cells were subjected to affinity purification using a Flag mAb, followed by SDS/PAGE and SYPRO Ruby staining. Several specific polypeptides were identified by mass spectrometry as described in *Materials and Methods*. (*B*) The 3xFlag–Gata3-expressing D10G4.1 cells were treated with or without formaldehyde as indicated (Cross-link + or –) before extraction. The extracts were then immunoprecipitated (I.P.) with a Flag mAb, followed by immunoblotting (I.B.) with an Ruvbl2 Ab (*Upper*). Total lysates were also subjected to I.B. in parallel (*Lower*). (*C*) The 293T cells were transfected with expression plasmids encoding Flag-tagged Gata3 and Myc-tagged Ruvbl2. Two days later, the extracts were I.P. with a Flag mAb, followed by I.B. with a Myc mAb (*Upper*). The total lysates were also subjected to I.B. in parallel (*Lower*). (*D*) GST or GST–Gata3 proteins were bound to glutathione Sepharose 4B and incubated with purified Myc-tagged Ruvbl2. The bound proteins were subjected to I.B. with an anti-Myc mAb (*Upper*). The inputs represent 10% of the amount of protein used in the pull-down sample (*Lower*). Three (C) and two (*B* and *D*) independent experiments were performed, and similar results were obtained.

Ruvbl2 Regulates the Proliferation of Th2 Cells. To identify the function of Ruvbl2 in differentiating Th2 cells, carboxyfluorescein diacetate succinimidyl ester (CFSE)-labeled naive CD4 T cells were transfected with Ruvbl2 siRNA and were cultured under Th2 conditions in vitro. The cell division was significantly inhibited in the Ruvbl2 knockdown (KD) cells, which was accompanied by decreased generation of IL-4–producing Th2 cells (Fig. 2*A*). Ruvbl2 KD had no impact on the mRNA or protein expression of Gata3 although efficient silencing of *Ruvbl2* mRNA expression was detected (Fig. S2 *A* and *B*). OX40-Cre–driven conditional *Gata3* knockout (*Gata3*-deficient) Th2 cells showed a similar phenotype as the Ruvbl2 KD Th2 cells (Fig. 2*B*). A substantial reduction in BrdU incorporation was observed in the Ruvbl2 KD Th2 cells (42.8% versus 21.6%) and also in *Gata3*-deficient Th2 cells (49.6% versus 34.5%) (Fig. 2*C*). These results indicate that Ruvbl2 and Gata3 positively regulate the proliferation of Th2 cells.

The Expression of *Cdkn2c* Is Repressed in a Gata3- and Ruvbl2-Dependent Manner. Earlier reports demonstrated that Gata3 regulates cell cycle in luminal progenitor cells and neuroblastoma cell via control of *Cdkn2c* and *Ccnd1* expression, respectively (19, 21). Thus, we next assessed the expression of *Cdkn2c* and *Ccnd1* in primary Th1 and Th2 cells from wild-type or *Gata3*-deficient mice. Although *Ccnd1* expression was not detected in primary Th1 and Th2 cells, the expression of *Cdkn2c* was lower in Th2 cells compared with Th1 cells, and the depletion of *Gata3* in Th2 cells resulted in increased expression of *Cdkn2c* (Fig. 3*A*). Moreover, the *Cdkn2c* expression was upregulated in primary Th2 cells when Ruvbl2 was silenced by siRNA (Fig. 3*B*). These results indicate that the expression of *Cdkn2c* is repressed in primary Th2 cells in a Gata3- and Ruvbl2-dependent manner.

To identify Gata3-bindng sites around the *Cdkn2c* locus, we performed a chromatin immunoprecipitation assay, followed by a massive parallel sequencing (ChIP-Seq) analysis using 3xFlag–Gata3-expressing Th2 clone cells (D10G4.1). Statistics of the tags generated for the experiment are summarized in Fig. S3*A*. The binding of 3xFlag-Gata3 at the previously validated Gata3-binding sites (Th2 cytokine and *Ccr8* loci) was confirmed (Fig. S3 *B* and *C*) (10, 11). From our ChIP-seq dataset, we identified two Gata3-binding sites around the *Cdkn2c* locus (Intron2 and +7.5-kb regions) (Fig. S3*D*, *Upper*). In the differentiating Th2 cells, Gata3 binding was detected only at the downstream region (+7.5 kb) of the *Cdkn2c* locus (Fig. 3*C*). Consistent with our results, the strongest binding of Gata3 at the +7.5-kb region of *Cdkn2c* was observed in primary Th2 cells compared with Th1 and Th17 cells in the previously reported ChIP-seq analysis for endogenous Gata3 (Fig. S3*D*, *Lower*) (11). We named the +7.5-kb region the Gata3 binding site (G3BS). To assess whether the G3BS plays a functional role in the Gata3-dependent transcriptional repression of *Cdkn2c*, a 500-bp fragment spanning the *Cdkn2c* G3BS (+7,261 ~ +7,760) (Fig. S4) was placed at the 5′-end of the *Cdkn2c* promoter (−500), and luciferase reporter assays were performed (Fig. 3*D*). The introduction of the G3BS substantially repressed the transcriptional activity of the *Cdkn2c* promoter whereas insertion of a G3BS with three mutations at the GATA consensus binding sequence did not show any effects (Fig. 3*D* and Fig. S4). These results indicate that Gata3 binds directly to the *Cdkn2c* locus and represses the mRNA expression of *Cdkn2c*.

Knockdown of *Cdkn2c* Expression Rescued the Impaired Proliferation of *Gata3*-Deficient Th2 Cells. Next, we examined whether Cdkn2c plays an important role in the Gata3-mediated induction of Th2 cell proliferation. Naive CD4 T cells from *Gata3*-deficient mice were stimulated under Th2 conditions for 2 d; then, the cells were infected with a retroviral vector containing shRNA specific for *Cdkn2c*. Four days after infection, the increased *Cdkn2c* mRNA expression in *Gata3*-deficient Th2 cells was abrogated in

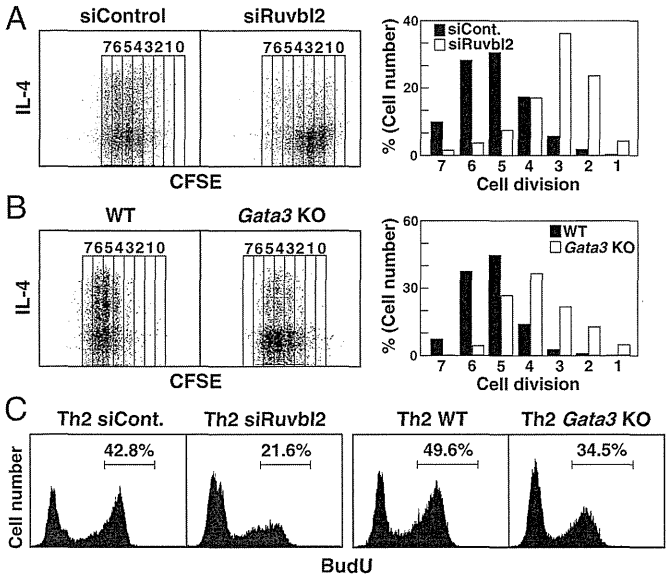

Fig. 2. Ruvbl2 regulates the proliferation of Th2 cells. (*A*) A control or Ruvbl2 siRNA was transfected into naive CD4 T cells, and the cells were labeled with CFSE. Then, the cells were stimulated with an immobilized anti-TCRβ mAb and anti-CD28 mAb under Th2 conditions for 3 d. The cells were then restimulated and subjected to intracellular staining with an APC-conjugated anti–IL-4 mAb (*Left*). The percentages of the cells in the gates representing the number of cell divisions (nos. 1 to 7) are shown (*Right*). (*B*) Naive CD4 T cells from WT or *Gata3*-deficient mice were labeled with CFSE and cultured under Th2 conditions for 3 d. The cells were then restimulated and subjected to IL-4 staining (*Left*). The percentages of the cells in the gates are shown (*Right*). (*C*) A control or Ruvbl2 siRNA was transfected into naive CD4 T cells, and the cells were stimulated with an immobilized anti-TCRβ mAb and anti-CD28 mAb under Th2 conditions for 4 d (*Left*). Naive CD4 T cells from WT or *Gata3*-deficient mice were cultured under Th2 conditions for 5 d (*Right*). Representative intracellular staining profiles for BrdU are shown with the percentages of cells in the gate. Three independent experiments were performed and similar results were obtained (*A*, *B*, and *C*).

the cells in which shCdkn2c had been introduced (Fig. 3*E*). We also found that the decreased BrdU incorporation and cell division in the *Gata3*-deficient Th2 cells compared with WT cells was restored by the introduction of shCdkn2c (Fig. 3 *F* and *G*). Interestingly, the restoration in IL-4 production was not observed by introduction of shCdkn2c in *Gata3*-deficient Th2 cells (Fig. 3*H*). These results indicate that Cdkn2c is specifically critical for the Gata3-mediated induction of the proliferation of Th2 cells.

The Transactivation Domain of Gata3 Is Required for the Association with Ruvbl2 and the Repression of *Cdkn2c* Expression. The GATA family transcriptional factors (Gata1 to -6) typically bind to a consensus motif (A/T)GATA(A/G) and regulate the specification and differentiation of numerous tissues. All GATA family members share two highly conserved C2H2-type zinc fingers, both of which are involved in DNA binding and protein–protein interactions (22, 23). Two transactivation domains are also known to be important for the function of Gata3 (24).

We examined which domains of Gata3 were important for the binding to Ruvbl2. Flag-tagged wild-type or deletion mutants of Gata3 (as depicted in Fig. S5 *A*, *Upper* and *B*, *Upper*) were cotransfected with Myc-tagged Ruvbl2 into 293T cells; then, the interaction was assessed by immunoprecipitation with a Flag mAb and subsequent immunoblotting with a Myc mAb. The association with Ruvbl2 was almost completely abrogated by the deletion of amino acids 65–178 (dTA), which is the region around the two transactivation domains of Gata3 (Fig. S5 *A* and *B*), thus indicating that the transactivation domains of Gata3 are important for binding to Rubvl2. To further examine whether these regions of Gata3 are important for the expression of *Cdkn2c*, we generated a stable Gata3 knockdown T-cell line. shRNAs against Gata3 or Ruvbl2 were introduced into a mouse T-cell line 68–41 using a lentivirus system. As expected, the expression of *Cdkn2c* was up-regulated in the Gata3 or Ruvbl2 knockdown 68–41 cells (Fig. S5*C*). We then expressed WT or dTA mutant Gata3 in these Gata3 knockdown 68–41 cells using a retrovirus system. Both the WT and dTA mutant Gata3 were substantially expressed in the Gata3 knockdown 68–41 cells (Fig. S5*D*, *Upper*). As shown in Fig. S5*D*, *Lower*, WT Gata3 repressed the *Cdkn2c* expression whereas the dTA mutant did not repress the expression of *Cdkn2c*. These results indicate that the transactivation domain of Gata3 is required for the repression of *Cdkn2c* expression.

Ruvbl2 Is Necessary for the Recruitment of Gata3 to the *Cdkn2c* Locus in Th2 Cells. To further investigate the molecular requirements for the Gata3-mediated repression of *Cdkn2c* expression in primary T cells, we used differentiating Th2 cells from *Gata3*-deficient mice. The introduction of WT Gata3 reduced the expression of *Cdkn2c* whereas the dTA mutant did not show any effect in the *Gata3*-deficient Th2 cells (Fig. 4*A*). The binding of the Gata3 dTA mutant to the *Cdkn2c* G3BS region was significantly compromised (Fig. 4*B*, *Left*). In contrast, the binding of the Gata3 dTA to the Th2 cytokine gene loci at the CGRE region was not compromised (Fig. 4*B*, *Right*), thus indicating that the Gata3 dTA mutant had a preserved DNA binding activity. In addition, a ChIP assay for endogenous Gata3 revealed that the Gata3 binding at the *Cdkn2c* G3BS region was impaired in Ruvbl2 KD Th2 cells (Fig. 4*C*). Thus, Ruvbl2 appears to regulate the binding of Gata3 to the *Cdnk2c* G3BS region in Th2 cells. Taken together, these results suggest that the association of Ruvbl2 with Gata3 is required for the binding of Gata3 to the *Cdkn2c* G3BS region.

Repressive Histone Modifications at the *Cdkn2c* Locus Induced by the Expression of Gata3 and Ruvbl2. We previously reported that the polycomb group (PcG) gene product, Bmi1, associates with Gata3 and controls the stability of the Gata3 protein in Th2 cells (25). In addition, Ruvbl2 was previously shown to be a component of the PcG complex in *Drosophila* (26, 27). Thus, we next investigated the histone modifications at the *Cdkn2c* locus, particularly histone H3-K27 trimethylation (H3-K27 Me3) and H2A-K119 monoubiquitination (H2A-K119 Ub), which are repressive marks known to be induced by PcG complexes. Interestingly, the H3-K27 Me3 and H2A-K119 Ub signals at the *Cdkn2c* locus, including the promoter, intron2, and G3BS regions, were higher in Th2 cells compared with Th1 and *Gata3*-deficient Th2 cells (Fig. 4 *D* and *E*). In addition, as shown in Fig. 4*F*, these histone modifications at the *Cdkn2c* promoter were significantly reduced in Ruvbl2 KD Th2 cells. Thus, repressive histone modifications at the *Cdkn2c* locus correlate strongly with both Gata3 and Ruvbl2 expression.

The Role of Ruvbl2 in Antigen-Induced Expansion of Th2 cells and Subsequent Induction of Allergic Airway Inflammation in Vivo. Finally, we investigated the in vivo physiological role of Ruvbl2 using a Th2 cell-dependent allergic airway inflammation model (28). Ruvbl2 KD Th2 cells or control cells generated by in vitro culture from DO11.10 Tg mice were i.v. injected into normal BALB/c mice. The mice were challenged twice by inhalation with 1% (wt/vol) OVA (Fig. S6). Before inhalation, control and Ruvbl2 KD Th2 cells were similarly detectable in the lung (Fig. 5*A*). A dramatic increase in the number of transferred Th2 cells ($KJ1^+$ cells) was induced by OVA inhalation (Fig. 5*A*, *Right*, black bars), and the increase was significantly impaired when Ruvbl2 was knocked down (Fig. 5*A*, *Right*). A significant decrease in the infiltration of inflammatory cells, including eosinophils, in the

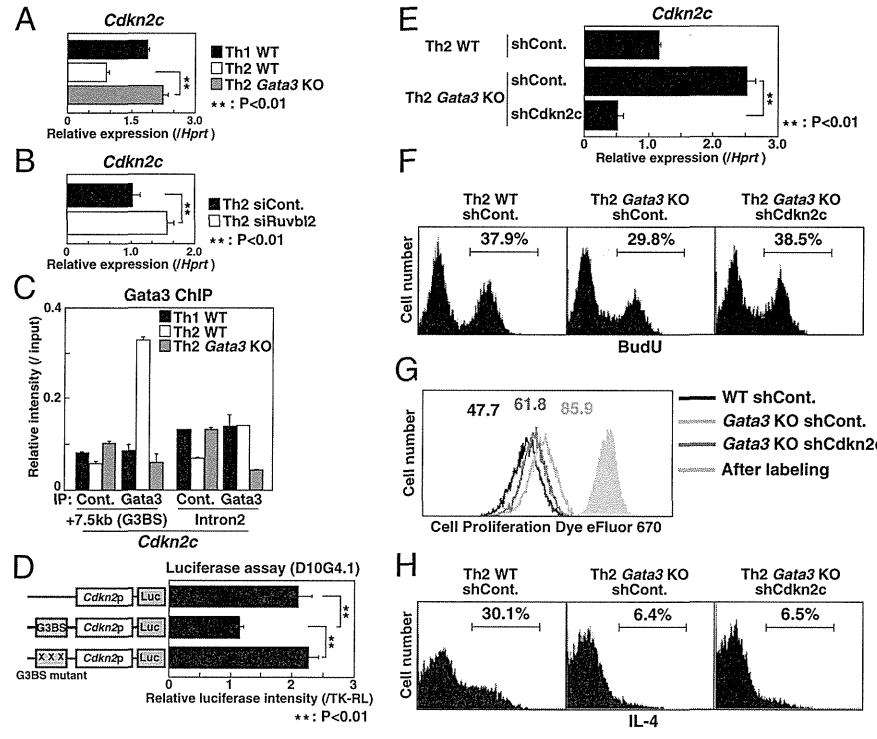

Fig. 3. The expression of *Cdkn2c* controls the Gata3-dependent proliferation of Th2 cells. (*A*) Naive CD4 T cells from either WT or *Gata3*-deficient mice were cultured under Th1 or Th2 conditions for 5 d, and the expression levels of *Cdkn2c* mRNA in Th1 WT, Th2 WT, or Th2 *Gata3* KO cells were determined by RT-qPCR. The relative expression (/*Hprt*) is shown with SDs. $^{**}P < 0.01$ by Student *t* test. (*B*) Naive CD4 T cells were transfected with control or Ruvbl2 siRNA, and cultured under Th2 conditions for 4 d; then, the expression levels of *Cdkn2c* mRNA were determined by RT-qPCR. (*C*) Naive CD4 T cells from WT or *Gata3*-deficient mice were cultured under Th1 or Th2 conditions for 3 d. The binding of Gata3 to the *Cdkn2c* locus was determined by a ChIP assay with a qPCR analysis. The relative intensities (/input) are shown with SDs. (*D*) D10G4.1 cells were transfected with the indicated reporter constructs. Two days after transfection, the cells were assayed for luciferase activity. The data indicate the mean values of three independent experiments with SDs. (*E*) Naive CD4 T cells from WT or *Gata3*-deficient mice were cultured under Th2 conditions for 2 d and then infected with a retroviral vector encoding a control shRNA or shCdkn2c bicistronically with a GFP gene. Four days later, the retrovirus-infected GFP-expressing cells were purified, and the levels of *Cdkn2c* mRNA were measured by RT-qPCR. (*F*) The BrdU incorporation in a portion of the same cultured cells used in *E* was determined. (*G*) The same cultured cells used in *E* were labeled with Cell Proliferation Dye eFluor 670 on day 3 after stimulation. Two days later, cell division was assessed by FACS. Numbers represent mean fluorescent units. (*H*) The same cultured cells used in *E* were stimulated with immobilized TCRβ mAb and subjected to IL-4 staining, followed by FACS analysis. The percentages of IL-4-producing cells are shown. Four (*A*), three (*B*, *C*, *E*, and *F*), and two (*D*, *G*, and *H*) independent experiments were performed, and similar results were obtained.

bronchioalveolar lavage (BAL) fluid was observed in the Ruvbl2 KD group in comparison with the control group (Fig. 5*B*). Histological analysis showed that mononuclear cell infiltration into the peribronchiolar regions of the lung was also modest in the Ruvbl2 KD animals (Fig. 5*C*, *Upper*). The levels of mucus hyperproduction and Goblet-cell metaplasia assessed by PAS staining were lower in the bronchioles of the Ruvbl2 KD group (Fig. 5*C*, *Lower*). These results indicate that Ruvbl2 regulates antigen-induced Th2 cell expansion and subsequent induction of allergic airway inflammation in vivo.

Discussion

We have herein identified a mechanism by which Gata3 facilitates the proliferation of differentiating Th2 cells. Gata3 associates with Ruvbl2 to form a unique repressive complex and represses the expression of a CDK inhibitor, *Cdkn2c*, via direct binding to the downstream region of the *Cdkn2c* gene (Fig. S7*B*). The discovery of the unique repressive Gata3/Ruvbl2 complex and the critical role of Ruvbl2 in the repression of *Cdkn2c* expression allow for mechanistic insight into the process of Th2-cell differentiation and proliferation.

Cdkn2c is a gene encoding p18 (ink4c), a member of the Ink4 family of cyclin-dependent kinase inhibitors. Ink4 family proteins bind to Cdk4 and Cdk6 to prevent the assembly of catalytically active cyclin D–CDK4/6 complexes and block the G1-S phase transition (17). Our results are consistent with the observation that *Cdkn2c*-deficient mice showed a hyperproliferative phenotype in response to TCR stimulation (18). In luminal progenitor cells, Gata3 was shown to directly bind to the promoter and intron of *Cdkn2c* and repress its expression to regulate the cell cycle (19). In addition, the involvement of Gata3 in the activation of Cyclin D1 (encoded by *Ccnd1*) in neuroblastoma cell lines and cell cycle entry in long-term repopulating hematopoietic stem cells were reported in previous studies (21, 29). Therefore, Gata3 appears to regulate the proliferation of various cell types through several distinct mechanisms.

Ruvbl2, a paralogue of Ruvbl1, was identified independently in multiple organisms and is implicated in many cellular pathways. Ruvbl1 and Ruvbl2 were both initially found as proteins that interacted with the TATA-box binding protein (Tbp) in *Drosophila*, yeast, and humans (30, 31). Ruvbl1 and Ruvbl2 belong to the AAA^+ (ATPase associated with multiple activities) ATPase family, have an ATPase domain with Walker A and Walker B motifs, and are conserved in different species. Ruvbl1 and Ruvbl2 are involved in the transcription of over 5% of yeast genes, many of which are directly involved in cell-cycle regulation (32). In addition to Tbp, the Ruvbl1 and Ruvbl2 have also been found to interact with various transcription factors, including c-Myc, β-catenin, and E2f, all of which are critical in the regulation of cell growth, proliferation, and apoptosis (30, 31). Previous reports have identified Ruvbl2 in various chromatin remodeling complexes, such as Tip60, Swr1, Baf, Ino80, and PcG molecule complexes. Moreover, mice heterozygous for a *Ruvbl2* mutation showed impaired T-cell development and maximal T-dependent antibody responses (33). The expression of *Ruvbl2* thus appears to play a critical role in the expansion of T cells in vivo.

Because Gata3 binding to the *Cdkn2c* locus is significantly lower in the absence of Ruvbl2, Gata3-mediated repression of *Cdkn2c* expression is dependent on Ruvbl2–Gata3 interaction (Fig. 4 and Fig. S5). With regard to the mechanisms by which Ruvbl2 controls Gata3 binding to the *Cdkn2c* locus, two possibilities should be considered. One is that the association of Gata3 with Ruvbl2 has an effect on the DNA binding activity of Gata3, and the other is that Ruvbl2 recruits chromatin-remodeling complexes altering the accessibility of the *Cdkn2c* locus to Gata3 (31). The binding of the Ruvbl2 to the *Cdkn2c* locus was comparable in Th1 and Th2 cells (Fig. S7*A*), indicating that the binding of Ruvbl2 to the *Cdkn2c* locus is Gata3-independent.

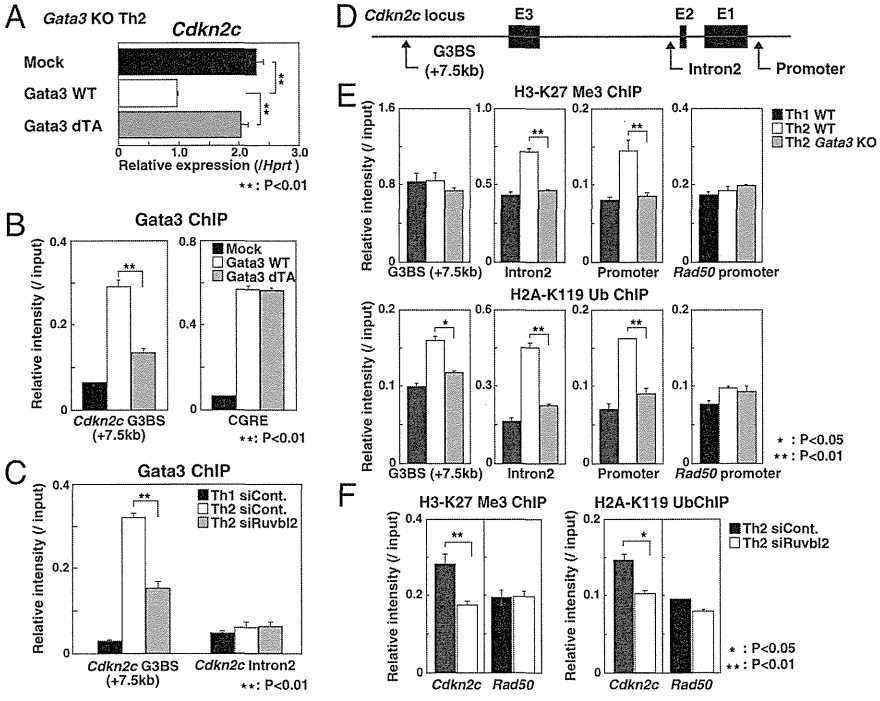

Fig. 4. Ruvbl2 is necessary for the recruitment of Gata3 at the *Cdkn2c* locus in developing Th2 cells. (*A*) Naive CD4 T cells from *Gata3*-deficient mice were stimulated under Th2 conditions for 2 d and then infected with a retroviral vector carrying WT or mutant (dTA) Gata3 cDNAs. Three days later, the retrovirus-infected GFP-expressing cells were purified, and the levels of mRNA of *Cdkn2c* were measured by RT-qPCR. $^{**}P < 0.01$ by Student *t* test. (*B*) The binding of Gata3 WT or dTA to the *Cdkn2c* G3BS and Th2 cytokine loci (CGRE region) were determined by the ChIP assay with a qPCR analysis using the same cells shown in *A*. (*C*) A control or Ruvbl2 siRNA was transfected into naive CD4 T cells, and the cells were stimulated under Th1 or Th2 conditions for 3 d. The binding of Gata3 to the *Cdkn2c* locus was determined. (*D*) A schematic representation of the *Cdkn2c* locus. The locations of primers and exons are indicated. (*E*) Naive CD4 T cells from WT or *Gata3*-deficient mice were cultured under Th1 or Th2 conditions for 5 d. The status of H3-K27 Me3 and H2A-K119 Ub at the *Cdkn2c* and *Hprt* loci was determined by a ChIP assay, using specific primers to detect the indicated regions. $^{**}P < 0.01$, $^{*}P < 0.05$ by Student *t* test. (*F*) A control or Ruvbl2 siRNA was transfected into naive CD4 T cells, and the cells were stimulated under Th2 conditions for 4 d. The status of H3-K27 Me3 and H2A-K119 Ub at the *Cdkn2c* and *Hprt* promoters was determined by a ChIP assay. Four (*A*), three (*B* and *C*), and two (*E* and *F*) independent experiments were performed, and similar results were obtained.

Thus, our findings may support the latter hypothesis, Ruvbl2 might associate with Gata3 at the *Cdkn2c* locus to facilitate and stabilize the DNA binding of Gata3 (Fig. S7*B*).

The recent genome-wide analyses indicated that GATA family transcription factors mediate both activating and repressive gene regulation (10, 11, 34–36). Interestingly, most of the GATA

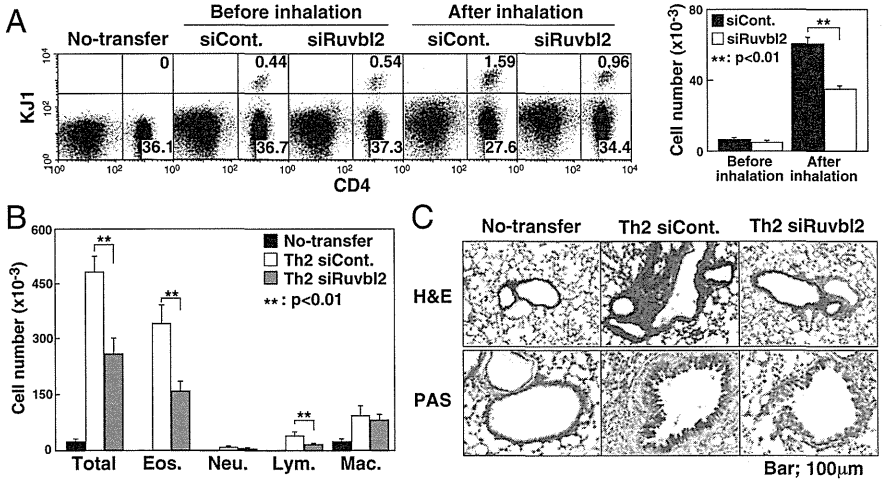

Fig. 5. Ruvbl2 regulates OVA-induced Th2 cell expansion and allergic airway inflammation in vivo. (*A*) A control or Ruvbl2 siRNA was transfected into naive CD4 T cells from DO11.10 Tg mice, and the cells were stimulated under Th2 conditions. On day 4, cells were i.v. transferred into BALB/c mice, and the mice were challenged with aerosolized OVA on days 5 and 7. Cells from lung were stained with antibodies against CD4 and KJ1.26 and assessed by FACS on days 5 (before inhalation) and 9 (after inhalation). A summary of the numbers of $KJ1^+$ cells in the lung is presented (*Right* graph). Four mice per group were used. $^{**}P < 0.01$ by Student *t* test. (*B*) The number of inflammatory cells in the bronchioalveolar lavage (BAL) fluid was counted. The absolute cell numbers of eosinophils (Eos.), neutrophils (Neu.), lymphocytes (Lym.) and macrophages (Mac.) are shown with SDs. Four mice per group were used. (*C*) The lungs were fixed and stained with hematoxylin/eosin (H&E) or with PAS. Representative staining patterns are shown. (Scale bar: 100 μm.) Two independent experiments were performed, and similar results were obtained (*A*, *B*, and *C*).

binding sites are localized at intragenic or intergenic regions where they can function as distal enhancers or silencers (11, 34–36). We have recently reported that Gata3 organizes a Gata3/Chd4/p300 activating complex at the enhancer regions of Th2 cytokine loci and a Gata3/Chd4-NuRD repressive complex at the intron 1 of *Tbx21* locus in Th2 cells and, thus, simultaneously positively regulates the expression of the Th2 cytokine genes and negatively regulates the *Tbx21* locus (37). In the current study, we found that Gata3 binds to the downstream region of the *Cdkn2c* locus (+7.5 kb from the transcriptional start site) and down-regulates the expression of *Cdkn2c* (Fig. 3). The introduction of a fragment spanning the *Cdkn2c* G3BS specifically repressed the transcriptional activity of the *Cdkn2c* promoter (Fig. 3*D*). Thus, the G3BS downstream of the *Cdkn2c* may have a Gata3-dependent intergenic silencer activity that affects the expression of *Cdkn2c*.

In summary, our results indicate that the Gata3/Ruvbl2 complex plays a crucial role in the regulation of Th2-cell proliferation by repressing the expression of a CDK inhibitor, *Cdkn2c*. This finding highlights a unique molecular mechanism that controls the process of the proliferation during Th-cell differentiation.

Materials and methods

Mice. C57BL/6 and BALB/c mice were purchased from CLEA Co. Conditional *Gata3*-deficient mice and OX40-Cre transgenic mice were kindly provided by Dr. William E. Paul (National Institutes of Health, Bethesda, MD) and Dr. Nigel Killeen (University of California, San Franciso, CA), respectively. Anti-ovalbumin (OVA)-specific TCR-αβ (DO11.10) transgenic (Tg) mice were provided by Dr. Dennis Loh (Washington University, St. Louis, MO). All mice were maintained under specific pathogen-free conditions and were used at 6–8 wk of age. All animal experiments were approved by the Chiba University Review Board for Animal Care.

The Generation of Th1 and Th2 Cells. Th1 and Th2 cells were generated as described previously (38). In brief, CD4 T cells with a naive phenotype ($CD44^{low}$) were purified using a FACSAria instrument (Becton Dickinson) yielding a purity of >98% and were stimulated with 3 μg/mL immobilized anti-TCRβ mAb plus 1 μg/mL anti-CD28 mAb under the Th1 or Th2 conditions in vitro.

Detailed descriptions of all materials and methods are provided in *SI Materials and Methods*.

ACKNOWLEDGMENTS. We thank Kaoru Sugaya, Hikari Kato, Terumi Horiuchi, Kayo Suzuki, and Toshihiro Ito for expert technical assistance. We also thank Dr. Yuka Kanno for critical suggestions on the manuscript. The lentivirus system was kindly provided by Dr. Hiroyuki Miyoshi (RIKEN BioResource Center). This work was supported by Global Center for Education and Research in Immune System Regulation and Treatment (Ministry of Education, Culture, Sports, Science and Technology, Japan) Grants-in-Aid Innovative Areas "Genome Science" 221S0002, "Crosstalk Between Transcription Control and Energy Pathway" 24116506, Scientific Research (B) 21390147, 22300325, and 24390239, (C) 19659121, and Exploratory Research and Young Scientists (B) 20790367 and 23790522; the Takeda Science Foundation; the Sagawa Cancer Foundation; the Astellas Foundation for Research on Metabolic Disorders; the Naito Foundation Natural Science Scholarship; the Princess Takamatsu Cancer Research Foundation; NOVARTIS Foundation for Gerontologic Research; NOVARTIS Foundation for the Promotion of Science; the Uehara Memorial Foundation; and the Research Fund of the Mitsukoshi Health and Welfare Foundation.

1. Zhu J, Yamane H, Paul WE (2010) Differentiation of effector CD4 T cell populations. *Annu Rev Immunol* 28:445–489.
2. Reiner SL (2007) Development in motion: Helper T cells at work. *Cell* 129(1):33–36.
3. Kurata H, Lee HJ, O'Garra A, Arai N (1999) Ectopic expression of activated Stat6 induces the expression of Th2-specific cytokines and transcription factors in developing Th1 cells. *Immunity* 11(6):677–688.
4. Onodera A, et al. (2010) STAT6-mediated displacement of polycomb by trithorax complex establishes long-term maintenance of GATA3 expression in T helper type 2 cells. *J Exp Med* 207(11):2493–2506.
5. Yamashita M, et al. (2005) Ras-ERK MAPK cascade regulates GATA3 stability and Th2 differentiation through ubiquitin-proteasome pathway. *J Biol Chem* 280(33):29409–29419.
6. Shinnakasu R, et al. (2008) Gfi1-mediated stabilization of GATA3 protein is required for Th2 cell differentiation. *J Biol Chem* 283(42):28216–28225.
7. Hosoya T, Maillard I, Engel JD (2010) From the cradle to the grave: Activities of GATA-3 throughout T-cell development and differentiation. *Immunol Rev* 238(1):110–125.
8. Rothenberg EV, Scripture-Adams DD (2008) Competition and collaboration: GATA-3, PU.1, and Notch signaling in early T-cell fate determination. *Semin Immunol* 20(4): 236–246.
9. Ansel KM, Djuretic I, Tanasa B, Rao A (2006) Regulation of Th2 differentiation and Il4 locus accessibility. *Annu Rev Immunol* 24:607–656.
10. Horiuchi S, et al. (2011) Genome-wide analysis reveals unique regulation of transcription of Th2-specific genes by GATA3. *J Immunol* 186(11):6378–6389.
11. Wei G, et al. (2011) Genome-wide analyses of transcription factor GATA3-mediated gene regulation in distinct T cell types. *Immunity* 35(2):299–311.
12. Nakayama T, Yamashita M (2008) Initiation and maintenance of Th2 cell identity. *Curr Opin Immunol* 20(3):265–271.
13. Grogan JL, et al. (2001) Early transcription and silencing of cytokine genes underlie polarization of T helper cell subsets. *Immunity* 14(3):205–215.
14. Zhu J, et al. (2002) Growth factor independent-1 induced by IL-4 regulates Th2 cell proliferation. *Immunity* 16(5):733–744.
15. Zhu J, et al. (2004) Conditional deletion of Gata3 shows its essential function in T(H)1-T(H)2 responses. *Nat Immunol* 5(11):1157–1165.
16. Nagasawa M, Melamed I, Kupfer A, Gelfand EW, Lucas JJ (1997) Rapid nuclear translocation and increased activity of cyclin-dependent kinase 6 after T cell activation. *J Immunol* 158(11):5146–5154.
17. Ortega S, Malumbres M, Barbacid M (2002) Cyclin D-dependent kinases, INK4 inhibitors and cancer. *Biochim Biophys Acta* 1602(1):73–87.
18. Kovalev GI, Franklin DS, Coffield VM, Xiong Y, Su L (2001) An important role of CDK inhibitor p18(INK4c) in modulating antigen receptor-mediated T cell proliferation. *J Immunol* 167(6):3285–3292.
19. Pei XH, et al. (2009) CDK inhibitor p18(INK4c) is a downstream target of GATA3 and restrains mammary luminal progenitor cell proliferation and tumorigenesis. *Cancer Cell* 15(5):389–401.
20. Tanaka T, Ohkubo S, Tatsuno I, Prives C (2007) hCAS/CSE1L associates with chromatin and regulates expression of select p53 target genes. *Cell* 130(4):638–650.
21. Molenaar JJ, et al. (2010) Cyclin D1 is a direct transcriptional target of GATA3 in neuroblastoma tumor cells. *Oncogene* 29(18):2739–2745.
22. Bates DL, Chen Y, Kim G, Guo L, Chen L (2008) Crystal structures of multiple GATA zinc fingers bound to DNA reveal new insights into DNA recognition and self-association by GATA. *J Mol Biol* 381(5):1292–1306.
23. Lowry JA, Atchley WR (2000) Molecular evolution of the GATA family of transcription factors: conservation within the DNA-binding domain. *J Mol Evol* 50(2):103–115.
24. Yang Z, et al. (1994) Human GATA-3 trans-activation, DNA-binding, and nuclear localization activities are organized into distinct structural domains. *Mol Cell Biol* 14(3): 2201–2212.
25. Hosokawa H, et al. (2006) Regulation of Th2 cell development by Polycomb group gene bmi-1 through the stabilization of GATA3. *J Immunol* 177(11):7656–7664.
26. Qi D, Jin H, Lilja T, Mannervik M (2006) Drosophila Reptin and other TIP60 complex components promote generation of silent chromatin. *Genetics* 174(1):241–251.
27. Diop SB, et al. (2008) Reptin and Pontin function antagonistically with PcG and TrxG complexes to mediate Hox gene control. *EMBO Rep* 9(3):260–266.
28. Miki-Hosokawa T, et al. (2009) CD69 controls the pathogenesis of allergic airway inflammation. *J Immunol* 183(12):8203–8215.
29. Ku CJ, Hosoya T, Maillard I, Engel JD (2012) GATA-3 regulates hematopoietic stem cell maintenance and cell-cycle entry. *Blood* 119(10):2242–2251.
30. Huen J, et al. (2010) Rvb1-Rvb2: Essential ATP-dependent helicases for critical complexes. *Biochem Cell Biol* 88(1):29–40.
31. Jha S, Dutta A (2009) RVB1/RVB2: Running rings around molecular biology. *Mol Cell* 34(5):521–533.
32. Jónsson ZO, et al. (2001) Rvb1p and Rvb2p are essential components of a chromatin remodeling complex that regulates transcription of over 5% of yeast genes. *J Biol Chem* 276(19):16279–16288.
33. Arnold CN, et al. (2012) A forward genetic screen reveals roles for Nfkbid, Zeb1, and Ruvbl2 in humoral immunity. *Proc Natl Acad Sci USA* 109(31):12286–12293.
34. Yu M, et al. (2009) Insights into GATA-1-mediated gene activation versus repression via genome-wide chromatin occupancy analysis. *Mol Cell* 36(4):682–695.
35. Fujiwara T, et al. (2009) Discovering hematopoietic mechanisms through genome-wide analysis of GATA factor chromatin occupancy. *Mol Cell* 36(4):667–681.
36. He A, Kong SW, Ma Q, Pu WT (2011) Co-occupancy by multiple cardiac transcription factors identifies transcriptional enhancers active in heart. *Proc Natl Acad Sci USA* 108(14):5632–5637.
37. Hosokawa H, et al. (2013) Functionally distinct Gata3/Chd4 complexes coordinately establish T helper 2 (Th2) cell identity. *Proc Natl Acad Sci USA* 110(12):4691–4696.
38. Yamashita M, et al. (2006) Crucial role of MLL for the maintenance of memory T helper type 2 cell responses. *Immunity* 24(5):611–622.

Immunity
Article

The Polycomb Protein Ezh2 Regulates Differentiation and Plasticity of CD4$^+$ T Helper Type 1 and Type 2 Cells

Damon J. Tumes,[1] Atsushi Onodera,[1] Akane Suzuki,[1] Kenta Shinoda,[1] Yusuke Endo,[1] Chiaki Iwamura,[1] Hiroyuki Hosokawa,[1] Haruhiko Koseki,[2] Koji Tokoyoda,[1] Yutaka Suzuki,[3] Shinichiro Motohashi,[4] and Toshinori Nakayama[1,5,*]

[1]Department of Immunology, Graduate School of Medicine, Chiba University, 1-8-1 Inohana, Chuo-ku, Chiba 260-8670, Japan
[2]Laboratory for Developmental Genetics, RIKEN Center for Integrative Medical Sciences (IMS-RCAI), 1-7-22 Suehiro, Tsurumi-ku, Yokohama 230-0045, Japan
[3]Department of Medical Genome Sciences, Graduate School of Frontier Sciences, University of Tokyo, 5-1-5 Kashiwanoha, Kashiwa, Chiba 277-8562, Japan
[4]Department of Medical Immunology, Graduate School of Medicine, Chiba University, 1-8-1 Inohana, Chuo-ku, Chiba 260-8670, Japan
[5]JST, CREST, 1-8-1 Inohana, Chuo-ku, Chiba 260-8670, Japan
*Correspondence: tnakayama@faculty.chiba-u.jp
http://dx.doi.org/10.1016/j.immuni.2013.09.012

SUMMARY

After antigen encounter by CD4$^+$ T cells, polarizing cytokines induce the expression of master regulators that control differentiation. Inactivation of the histone methyltransferase Ezh2 was found to specifically enhance T helper 1 (Th1) and Th2 cell differentiation and plasticity. Ezh2 directly bound and facilitated correct expression of *Tbx21* and *Gata3* in differentiating Th1 and Th2 cells, accompanied by substantial trimethylation at lysine 27 of histone 3 (H3K27me3). In addition, Ezh2 deficiency resulted in spontaneous generation of discrete IFN-γ and Th2 cytokine-producing populations in nonpolarizing cultures, and under these conditions IFN-γ expression was largely dependent on enhanced expression of the transcription factor Eomesodermin. In vivo, loss of Ezh2 caused increased pathology in a model of allergic asthma and resulted in progressive accumulation of memory phenotype Th2 cells. This study establishes a functional link between Ezh2 and transcriptional regulation of lineage-specifying genes in terminally differentiated CD4$^+$ T cells.

INTRODUCTION

Upon encountering antigen, naive CD4$^+$ T cells differentiate into discrete subsets of effector T helper (Th) cells, a process controlled by the cytokines present during activation. Th cell subsets including Th1, Th2, Th9, and Th17 then induce different types of immune responses (Reiner, 2007; Zhu et al., 2010). Interferon gamma (IFN-γ)-producing Th1 cells are essential for immunity to intracellular pathogens, and interleukin 4 (IL-4)-, IL-5-, and IL-13-producing Th2 cells promote immunity to parasitic worms and also allergic inflammation. Expression of lineage-specifying transcription factors is required for Th cell differentiation. T-bet (encoded by *Tbx21*) can induce Th1 cell differentiation (Szabo et al., 2000), and Gata3 is required and sufficient for differentiation of Th2 cells (Yamashita et al., 2004; Zheng and Flavell, 1997). In addition, a transcription factor related to T-bet called Eomesodermin (Eomes) can also induce IFN-γ production in Th cells under some conditions (Suto et al., 2006; Tofukuji et al., 2012; Yang et al., 2008). Appropriate expression of these transcription factors and the effector cytokines they control is therefore essential for proper immunoregulation. Th1 and Th2 cell differentiation programs possess strong feed-forward mechanisms to maintain polarization (Hosokawa et al., 2013; Hwang et al., 2005; Usui et al., 2003) and are generally considered to represent stable lineages of differentiated effector cells. However, it is also becoming apparent that appreciable levels of functional plasticity exist among the Th cell subsets (Kanno et al., 2012; O'Shea and Paul, 2010).

Epigenetic histone modifications provide cells with the ability to maintain specific phenotypic traits independently of changes to the primary DNA sequence. Several epigenetic modifications have been found to correlate with gene expression in Th cells (Ansel et al., 2006; Kanno et al., 2012; Löhning et al., 2002; Nakayama and Yamashita, 2008; Wei et al., 2009), with repressed genes frequently associated with increased levels of trimethylation of lysine 27 on histone 3 (H3K27me3). Polycomb proteins form two major repressive complexes: polycomb repressive complex 1 (PRC1) and PRC2. Interestingly, CD4$^+$ T cells lacking the PRC1 proteins Mel-18, Bmi1, and Ring1B exhibited impaired differentiation into Th2 cells, partially because of failure of these cells to inhibit cell death pathways (Kimura et al., 2001; Suzuki et al., 2010; Yamashita et al., 2008) and also because of the roles of Bmi1 (Hosokawa et al., 2006) and possibly Mel-18 (Kimura et al., 2001) in stabilization of the Gata3 protein. The polycomb proteins Enhancer of Zeste Homolog 1 (Ezh1) and Ezh2 form two closely related PRC2 complexes that can trimethylate H3K27 and are required for maintenance of cellular identity at several stages of development (Di Meglio et al., 2013; Ezhkova et al., 2009; Hirabayashi et al., 2009; O'Carroll et al., 2001; Shen et al., 2008; Su et al., 2003). Ezh2 is highly expressed in CD4$^+$ T cells and binds to the Gata3 locus prior to Th2 cell differentiation (Onodera

et al., 2010). In addition, the position of Ezh2 occupancy at the *Il4* and *Il13* loci was found to spatially correlate with the presence of H3K27me3 in Th1 cells (Koyanagi et al., 2005). In contrast, it has been suggested that Ezh2 is important for efficient actin polymerization and TCR-induced proliferation of peripheral $CD4^+$ T cells, and this study detected no evidence of decreased H3K27me3 in unstimulated Ezh2-deficient $CD4^+$ T cells (Su et al., 2005). Additionally, an unconventional role for Ezh2 in the positive regulation of cytokine genes in Th cells has been suggested (Jacob et al., 2008). Thus, it remains unresolved whether Ezh2 retains its canonical role as a genetic repressor in $CD4^+$ T cells.

Here we show that Ezh2 has important functions as a repressor of gene expression during Th cell differentiation. Ezh2 bound strongly to genes encoding the transcription factors T-bet, Eomes, and Gata3, controlled differentiation into Th1 and Th2 effector cells, and regulated plasticity of these subsets after differentiation. In vivo, Ezh2-deficient ($Ezh2^{\Delta SET/\Delta SET}$) Th2 cells caused enhanced pathology in a mouse model of allergic asthma, and $CD4^+$-specific Ezh2 deficiency resulted in progressive accumulation of memory phenotype Th2 cells. These data indicate that Ezh2 plays an essential role in regulating both differentiation and stability of effector function in $CD4^+$ T cells.

RESULTS

The Histone H3K27 Methyltransferase Ezh2 Controls Differentiation of Th1 and Th2 Cells

To directly assess the role of Ezh2 during Th cell differentiation, we used mice in which the Ezh2 SET domain (responsible for H3K27 methyltransferase activity of Ezh2) was conditionally deleted (Hirabayashi et al., 2009) in $CD4^+$ T cells by expression of Cre-recombinase under control of the *Cd4* promoter (herein referred to as $Ezh2^{\Delta SET/\Delta SET}$ or Ezh2-deficient cells). The truncated Ezh2 ΔSET protein could be detected in $Ezh2^{\Delta SET/\Delta SET}$ $CD4^+$ T cells, but expression was much lower compared to the levels of native Ezh2 in wild-type (WT) cells (Figure S1A available online). Mice with $CD4^+$ T cell-specific Ezh2 deficiency (6 weeks old, young adult) had normal proportions of $CD4^+$ and $CD8^+$ T cells in the spleen and thymus (Figure S1B) and normal expression of T cell-associated surface markers on $CD4^+$ T cells (Figure S1C). In addition, we did not observe any defects in IL-2 production (Figure S1D) or initial proliferation of $Ezh2^{\Delta SET/\Delta SET}$ $CD4^+$ T cells (Figures S1E and S1F). We first investigated whether loss of Ezh2 could affect Th cell differentiation. Ezh2-deficient Th cells produced markedly more IFN-γ in cultures with titrated doses of the Th1 cell-inducing cytokine IL-12 (Figures 1A and 1C). Likewise, more IL-4, IL-5, and IL-13 were produced in cultures with the Th2 cell-inducing cytokine IL-4 (Figures 1B and 1D). Interestingly, enhanced IFN-γ production by Ezh2-deficient cells was still observed without addition of IL-12, and this could be inhibited by IL-4 (Figure 1B). In addition, compared to WT cells, increased amounts of IFN-γ, IL-4, IL-5, and IL-13 were produced by Ezh2-deficient $CD4^+$ T cells activated via the TCR without any exogenously added cytokines (Figure 1E). Importantly, as shown by intracellular staining, the majority of IFN-γ- and IL-4-producing cells were mutually exclusive, indicating that loss of Ezh2 does not disable Th cell polarization (Figures 1A and 1B). We also investigated the effect of 3-Deazaneplanocin A (DZNep), a specific inhibitor of histone methyltransferase activity. This agent has been shown to inhibit Ezh2 and reactivate polycomb repressed genes in cancer cells (Tan et al., 2007) and to preferentially decrease H3K27me3 in T lymphocytes (He et al., 2012). Treatment of $CD4^+$ T cells with low concentrations of DZNep (7.5 and 15 nM) during differentiation resulted in a dose-dependent increase in the production of IFN-γ or of IL-4, IL-5, and IL-13 under Th1 or Th2 cell-inducing conditions, respectively (Figures 1F and 1G). These data indicate that inhibition of Ezh2 activity via genetic inactivation or chemical inhibition strongly enhances cytokine production and differentiation of Th1 and Th2 cells.

Loss of Ezh2 Results in Enhanced Th1 and Th2 Cell Polarization with Increased Expression of T-bet and Gata3

To determine whether cytokine expression in Ezh2-deficient cells coincided with expression of lineage-specifying transcription factors at the single-cell level, we analyzed expression of T-bet together with IFN-γ and of Gata3 together with IL-4 (Figures 2A and 2B). Ezh2-deficient cells again showed markedly increased cytokine production. Importantly, those cells that produced IFN-γ also expressed higher amounts of T-bet, and the cells that produced IL-4 expressed higher amounts of Gata3. We also found enhanced expression of *Tbx21* and *Gata3* mRNA at all of the concentrations of polarizing cytokines tested (Figures 2C and 2D). To further analyze the contribution of T-bet to the enhanced IFN-γ production by Ezh2-deficient cells, we compared WT, $Tbx21^{-/-}$, $Ezh2^{\Delta SET/\Delta SET}$, and cells doubly deficient for Ezh2 and T-bet ($Ezh2^{\Delta SET/\Delta SET}Tbx21^{-/-}$) differentiated under Th1 cell-inducing conditions. We detected an approximate 50% reduction in IFN-γ production by $Tbx21^{-/-}$ Th1 cells compared to WT cells, and again IFN-γ production by $Ezh2^{\Delta SET/\Delta SET}$ cells was markedly enhanced. In double-deficient $Ezh2^{\Delta SET/\Delta SET}Tbx21^{-/-}$ cells, the enhanced IFN-γ production induced by loss of Ezh2 was substantially reduced (Figure 2E), indicating that the increased expression of IFN-γ in Th1 polarized Ezh2-deficient cells is largely dependent on T-bet. To assess the contribution of Gata3 to Th2 cytokine production, we used Gata3 siRNA to knock down Gata3 expression in Ezh2-deficient cells differentiated under Th2 cell polarizing conditions. Gata3 siRNA abolished IL-4, IL-5, and IL-13 production by Ezh2-deficient Th2 cells (Figure 2F). These data indicate that Gata3 is required for enhanced Th2 cytokine production in cells lacking Ezh2 and confirm that Ezh2-deficient cells are unable to bypass the requirement for Gata3 in Th2 cytokine expression. In contrast to the large enhancement of Th1 and Th2 cell differentiation, we detected only a very small increase in IL-17 production when comparing WT and Ezh2-deficient cells differentiated under Th17 cell-inducing conditions, and the expression of Rorγt was also only slightly increased (Figures S2A and S2B). In addition, we found no enhancement, but rather a decrease in differentiation into Th9 and iTreg cells by Ezh2-deficient $CD4^+$ T cells (Figures S2C and S2D). Interestingly, under Th17, Th9, and also iTreg cell-inducing conditions, we again detected more IFN-γ production by Ezh2-deficient cells compared to WT cells.

Genome-wide Analysis of Ezh2 Binding in Th1 and Th2 Cells

To globally determine the genes most likely to regulate the enhanced Th1 and Th2 cytokine production by Ezh2-deficient

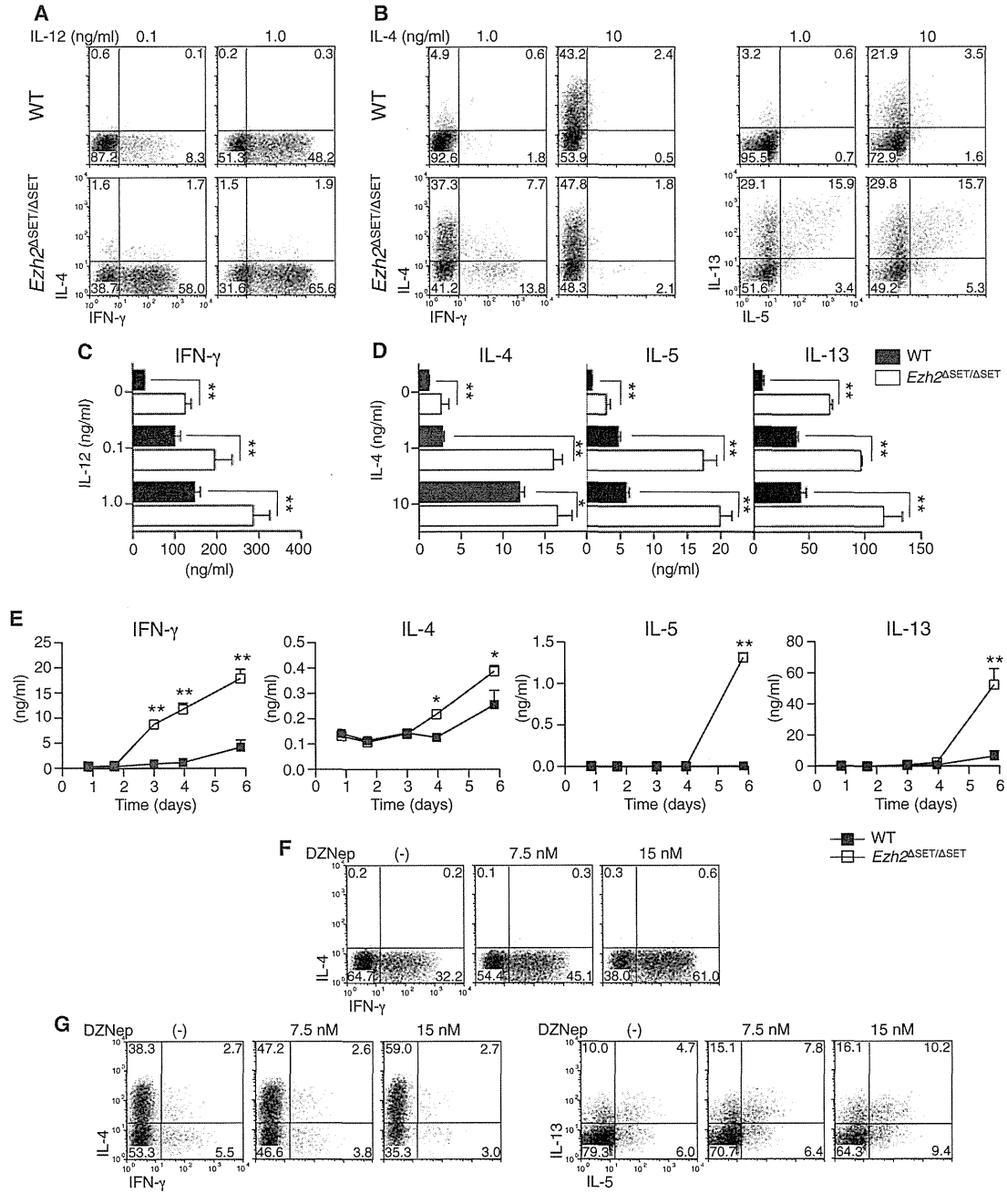

Figure 1. Loss of Ezh2 Function Results in Enhanced Th1 and Th2 Cell Differentiation

(A–D) Naive wild-type (WT) or Ezh2-deficient (*Ezh2*$^{\Delta SET/\Delta SET}$) CD4$^+$ T cells differentiated under Th1 (A and C) or Th2 (B and D) cell-inducing conditions with the indicated concentrations of IL-12 or IL-4, respectively.

(E) Naive CD4$^+$ T cells activated with anti-TCRβ alone for the indicated times.

(F and G) Naive CD4$^+$ T cells were cultured under Th1 cell-inducing conditions with 0.1 ng/ml IL-12 (F) or Th2 cell-inducing conditions with 1 ng/ml IL-4 (G) and the indicated concentrations of the Ezh2 inhibitor DZNep.

Cytokine production measured by cytoplasmic staining of IL-4 and IFN-γ or IL-5 and IL-13 after 5 hr restimulation with anti-TCRβ (A, B, F, and G) and ELISA after 24 hr restimulation with anti-TCRβ (C and D) or the indicated time of culture (E) (n = 3, mean ± SD). Data are representative of at least three independent experiments. *$p < 0.05$, **$p < 0.01$. See also Figure S1.

Th cells, we used transcriptional profiling of Ezh2-deficient Th cells combined with genome-wide mapping of Ezh2 target genes in WT Th1 and Th2 cells. Ezh2 deficiency resulted in 856 upregulated and 908 downregulated genes in nonpolarized Th cells. Gene ontology (GO) analysis (Huang et al., 2009) of the upregulated genes showed that the most statistically overrepresented

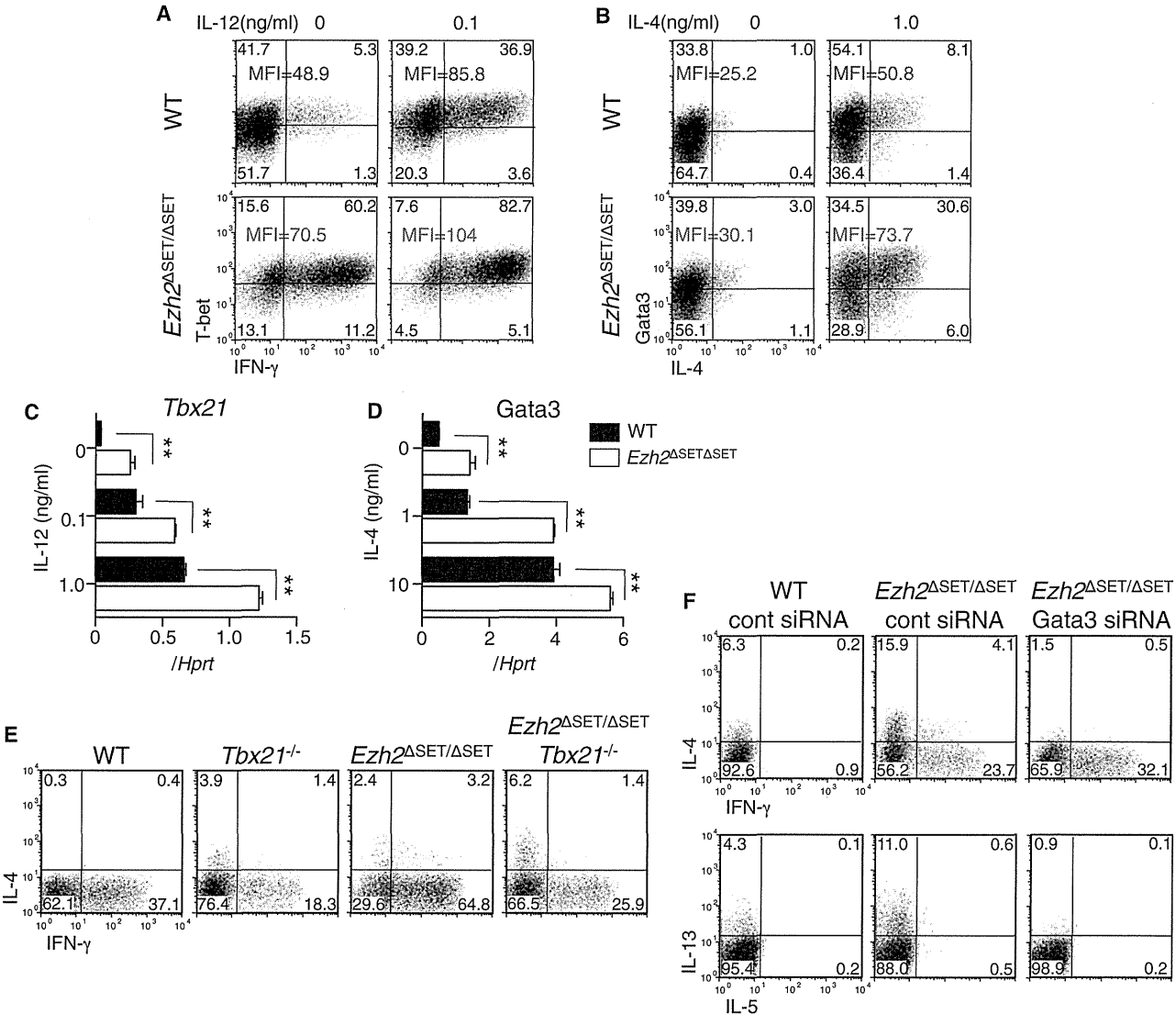

Figure 2. Loss of Ezh2 Results in Enhanced Expression of the Master Regulators T-bet and Gata3

(A–D) Naive WT or *Ezh2*$^{\Delta SET/\Delta SET}$ CD4$^+$ T cells differentiated under Th1 (A and C) or Th2 (B and D) cell-inducing conditions with the indicated concentrations of IL-12 or IL-4, respectively. mRNA expression of *Tbx21* (T-bet) (C) and *Gata3* (D), n = 3, mean ± SD. **p < 0.01.

(E) Naive WT, *Tbx21*$^{-/-}$, *Ezh2*$^{\Delta SET/\Delta SET}$, and *Ezh2*$^{\Delta SET/\Delta SET}$ *Tbx21*$^{-/-}$ double-deficient CD4$^+$ T cells differentiated under Th1 cell-inducing conditions with 0.1 ng/ml IL-12.

(F) Naive CD4$^+$ T cells differentiated under Th2 cell-inducing conditions with 1 ng/ml of IL-4 and electroporated with control siRNA (WT and *Ezh2*$^{\Delta SET/\Delta SET}$ cells) or Gata3 siRNA (*Ezh2*$^{\Delta SET/\Delta SET}$ cells).

Cytoplasmic staining of T-bet with IFN-γ (A) and Gata3 with IL-4 (B), mean fluorescence intensities (MFIs) of T-bet and Gata3 are shown (WT cells, blue; *Ezh2*$^{\Delta SET/\Delta SET}$ cells, red) and IL-4 with IFN-γ (E and F) and IL-5 with IL-13 (F). Data are representative of at least three independent experiments. See also Figure S2.

groups were involved in immune responses (immune system process; GOTERM_BP, $p = 1.5 \times 10^{-19}$, 96 genes), with approximately half encoding cytokines and their receptors (cytokine-cytokine receptor interaction; KEGG pathway, $p = 2.5 \times 10^{-13}$, 44 genes). This indicates that cellular context is important in determining which genes are derepressed when Ezh2 is absent, a phenomenon that has also been reported in other studies (Ezhkova et al., 2009; Hirabayashi et al., 2009). Of the genes defined in reference genome mm9 in the RefSeq database, 9.5% (1,998 genes) were bound by Ezh2 in both Th1 and Th2 cells, 1.1% (240 genes) were bound in Th1 cells only, and 2.0% (415 genes) were bound in Th2 cells only (Figure S3A). GO analysis of all bound genes showed very strong enrichment of genes involved in development (developmental process; GOTERM_BP, $p = 5.1 \times 10^{-117}$, 743 genes) and transcription (transcription factor activity; GOTERM_MF, $p = 1.1 \times 10^{-87}$, 308 genes), similar to that reported for polycomb proteins in embryonic stem cells (Boyer et al., 2006). Ezh2 binding was detected at 16.0% (137 of 856 genes) of the upregulated genes and also at 6.6% (60 of 908 genes) of the downregulated genes. Ezh2 binding was significantly more likely to be detected at genes upregulated in response to inactivation of Ezh2 (chi-square test,

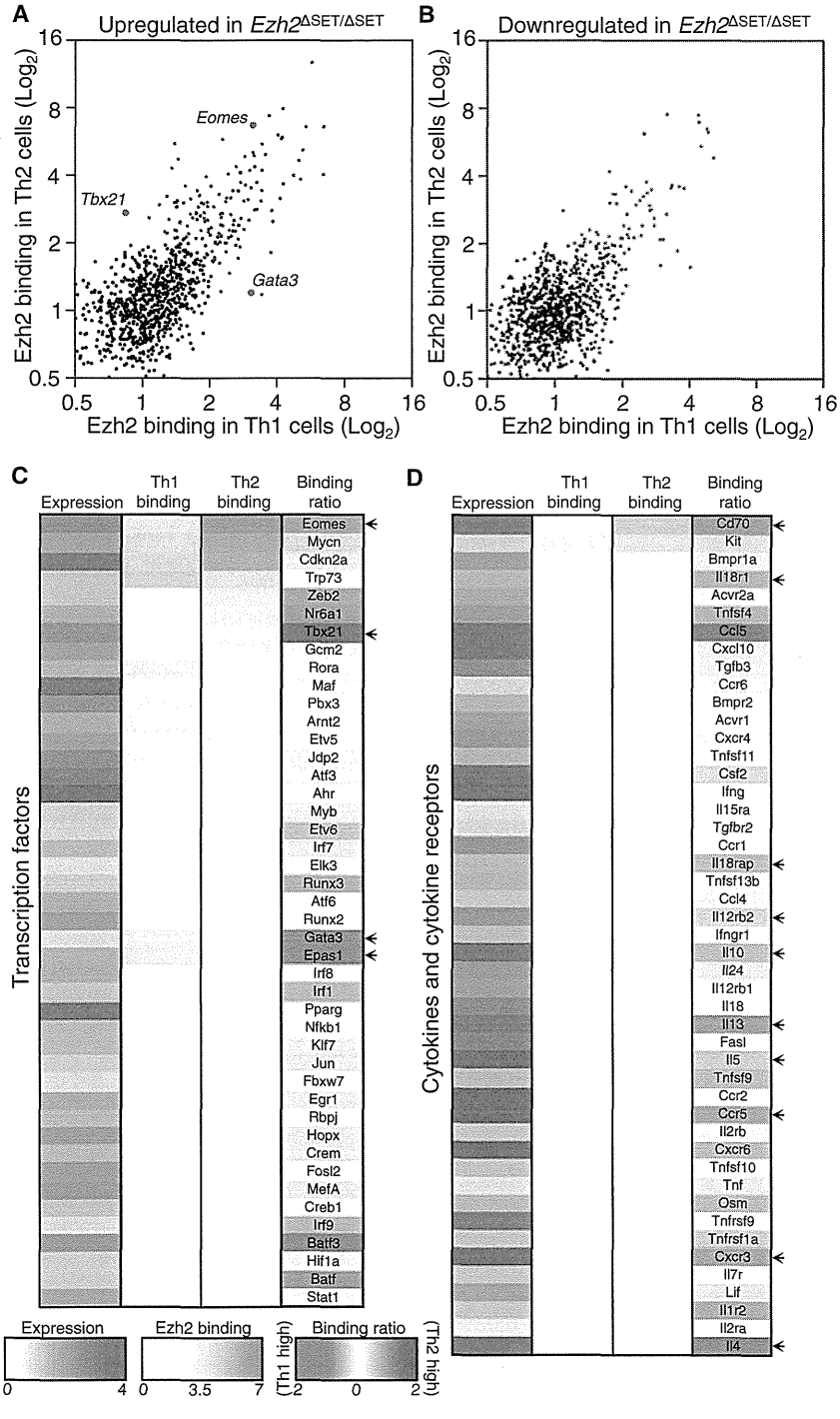

Figure 3. Global Analysis of Ezh2 Function and Localization by Gene Expression and ChIP-Seq Analysis

(A and B) Scatter plots depicting Ezh2 binding in Th1 cells (x axes) and Th2 cells (y axes) for all genes upregulated (A) and downregulated (B) in $Ezh2^{\Delta SET/\Delta SET}$ nonpolarized Th cells. Blue dots indicate greater than 2-fold enrichment of Ezh2 binding with *Tbx21*, *Eomes*, and *Gata3* (shown in red).

(C and D) Upregulated genes encoding transcription factors (C) and cytokines and cytokine receptors (D) in $Ezh2^{\Delta SET/\Delta SET}$ nonpolarized Th cells. Left column, fold upregulation (red); middle columns, Ezh2 binding in WT Th1 and Th2 cells (orange); right column, log2 ratio of Ezh2 binding between WT Th1 and Th2 cells (Th1 high, green; Th2 high, purple).

See also Figure S3.

$p = 7.3 \times 10^{-8}$); however, the presence of Ezh2 at a small subset of the downregulated genes also indicates that Ezh2 could play a more complex role in gene regulation at some loci. Ezh2 binding intensity in Th1 versus Th2 cells at all genes up- and downregulated by inactivation of Ezh2 are depicted; genes with more than 2-fold enrichment of Ezh2 are indicated in blue (Figures 3A and 3B and Table S1 and S2), with the transcription factors *Gata3*, *Tbx21*, and *Eomes* indicated in red. Based on our results by GO analysis, we then assessed the upregulated genes encoding transcription factors (44 genes) (Figure 3C) and cytokines and cytokine receptors (47 genes) (Figure 3D) in more detail. Overall, transcription factor genes showed significantly higher Ezh2 binding (Student's t test, $p = 0.003$). The lineage-specifying genes *Tbx21* and *Gata3*, and another gene with unknown function in Th1 or Th2 cells called *Epas1* (Figure 3C, arrows), showed the most dramatic changes in Ezh2 occupancy during differentiation. In Th1 cells, Ezh2 also preferentially bound genes encoding several cytokines produced by Th2 cells including IL-4, IL-5, IL-10, IL-13, and IL-24; however, Ezh2 occupancy at these loci was very low (Figure 3D, arrows). Loss of Ezh2 also resulted in increased expression of *Maf*, another transcription factor associated with regulation of Th2 cytokine expression; however, this gene did not appear to be a strong target of Ezh2, and there was no difference in Ezh2 binding at this loci in Th1 cells compared to Th2 cells (Figure S3B). As expected, no difference in Ezh2 binding between Th1 and Th2 cells was found at the *Ifng* gene; however, ChIP-seq analysis identified an area between 40 and 50 kb downstream of the *Ifng* gene that showed moderately higher Ezh2 binding in Th2 cells (Figure S3B), an area that may be functionally important for *Ifng* gene regulation (Schoenborn et al., 2007). We also found preferential Ezh2 binding in Th2 cells at genes encoding several surface receptors normally expressed on Th1 cells including *Cxcr3*, *Ccr5*, *Cd70*, *Il18r1*, *Il18rap*, and *Il12rb2* and the chemokine *Ccl5* (Figure 3D, arrows). Ezh2 ChIP-seq profiles for *Gata3*, *Epas1*, *Maf*, *Tbx21*, *Eomes*, Th2 cytokine, and *Ifng* loci are shown in Figure S3B. These data indicate that Ezh2 is dynamically regulated at several of the signature genes that define the Th1 and Th2 cell

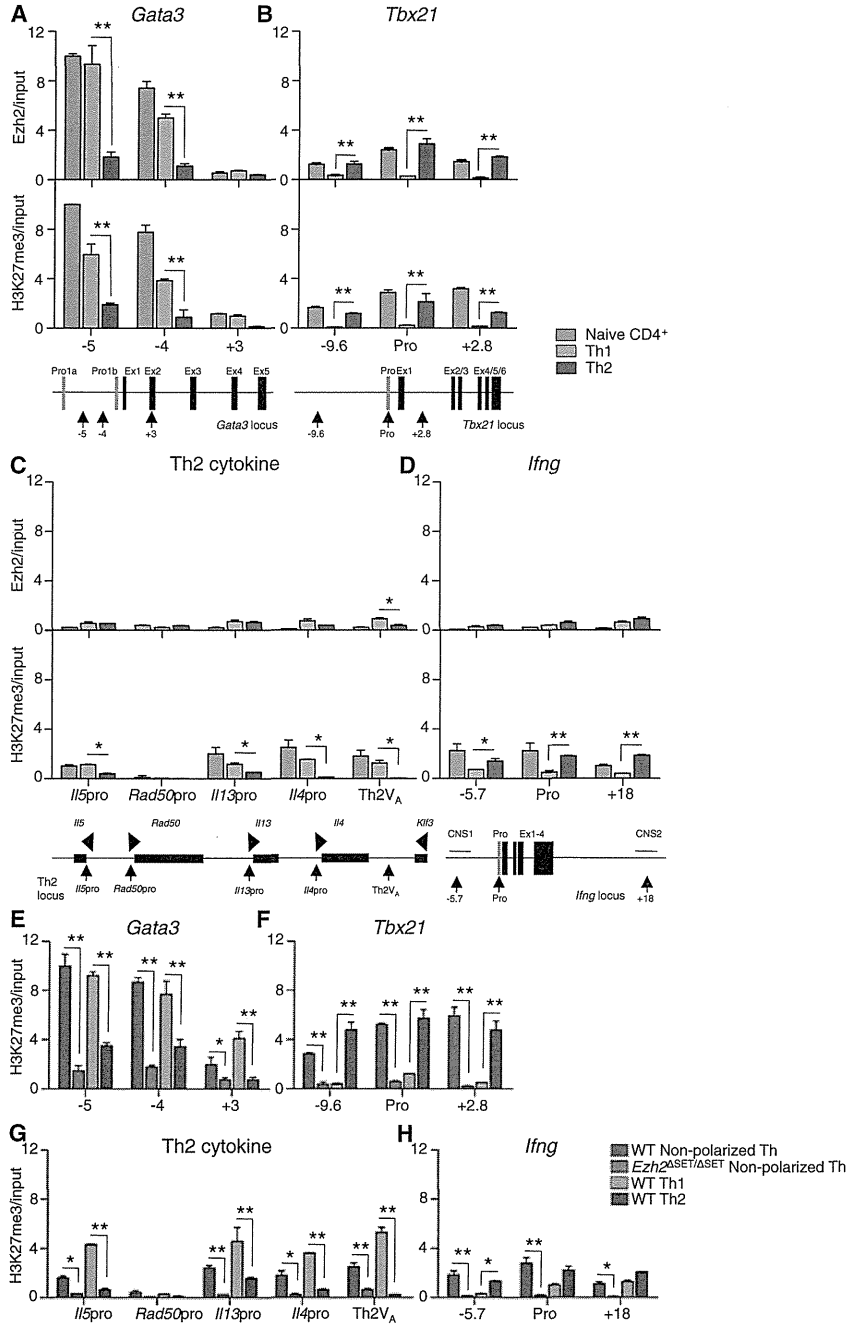

Figure 4. Dynamic Changes in Ezh2 Binding and H3K27me3 Occur during Th1 and Th2 Cell Differentiation

Ezh2-ChIP and H3K27me3-ChIP on WT CD4+ naive, Th1, and Th2 cells (A–D), and H3K27me3-ChIP on WT and *Ezh2*$^{\Delta SET/\Delta SET}$ nonpolarized Th cells with WT Th1 and Th2 cells for comparison (E–H), for *Gata3* (A and E), *Tbx21* (B and F), Th2 cytokine (C and G), and *Ifng* (D and H) loci measured by qPCR (n = 3, mean ± SD). Schematic representations of each gene loci show the positions of the primers used for detection relative to the transcriptional start site of each gene. Data are representative of three independent experiments. *p < 0.05, **p < 0.01; Abbreviation: pro., promoter. See also Figure S4.

differentiation programs. Moreover, it confirms that *Tbx21* and *Gata3* display comparatively stronger binding of Ezh2 and that these genes are among those that display the most dramatic differences in Ezh2 occupancy during differentiation.

Ezh2 Bound Directly to the Genes Encoding T-bet and Gata3 and Deficiency of Ezh2 Resulted in Loss of H3K27me3 at These Loci

To determine whether Ezh2 was lost after differentiation or recruited to *Gata3* and *Tbx21* loci, we performed ChIP on WT naive CD4+ T cells and differentiated Th1 and Th2 cells. Ezh2 binding was detected at the *Gata3* locus in naive and Th1 cells, which was dramatically diminished in Th2 cells (Figure 4A). A similar but reciprocal regulation was observed at the *Tbx21* locus where binding was detected in naive and Th2 cells but was absent in Th1 cells (Figure 4B). We also used H3K27me3-specific ChIP to assess the presence of the H3K27me3 modification at these loci in WT cells and found strong positive correlations between the level of Ezh2 binding and H3K27me3 (Pearson's correlation coefficient for *Gata3* locus r = 0.95, p < 0.0001 and *Tbx21* locus r = 0.77, p = 0.007) (Figures 4A and 4B). In agreement with the ChIP-seq data, we detected relatively little Ezh2 binding at the Th2 and *Ifng* cytokine loci compared to that observed for *Gata3* and *Tbx21* (Figures 4C and 4D). Interestingly, we did detect H3K27me3 associated with the Th2 and *Ifng* cytokine loci (Figures 4C and 4D), and H3K27me3 was lost at the Th2 cytokine loci in Th2 cells and at the *Ifng* locus in Th1 cells. At the *Rad50* promoter, an unrelated gene within the Th2 cytokine loci, we did not detect any differences in Ezh2 occupancy or H3K27me3 (Figure 4C), nor did we detect any differences in total H3 during differentiation at any of these genes (data not shown). Therefore, at the *Gata3* and *Tbx21* loci, differential binding of Ezh2 and the associated H3K27me3 modification in differentiated cells appears to be accomplished primarily via loss of high levels of pre-existing Ezh2 in naive CD4+ T cells. In contrast, both Ezh2 and H3K27me3 are maintained during the process of activation and cell division at lineage-specifying genes of the opposing Th cell subtype. Compared to the *Gata3* locus, Ezh2 occupancy and H3K27me3 at the *Il17a* and *Rorc* loci in Th cells activated without polarizing cytokines and in Th cells polarized under Th17 cell-inducing conditions were very low (Figure S4A). As

expected, association of Ezh2 with the *Gata3* and *Tbx21* loci was dramatically reduced in *Ezh2*$^{\Delta SET/\Delta SET}$ Th cells (Figures S4B and S4C). To determine whether a functional link exists between the presence of Ezh2 and H3K27me3, we assessed H3K27me3 at the *Gata3, Tbx21*, Th2, and *Ifng* cytokine loci. In nonpolarized Ezh2-deficient cells, we found that H3K27me3 was depleted at both transcription factor and cytokine loci, indicating that Ezh2 was required for the presence of H3K27me3 at both transcription factor and cytokine genes (Figures 4E–4H).

Ezh2-Mediated Repression of T-bet and Eomes Is Required to Control Spontaneous Generation of IFN-γ-Producing T Cells

Enhanced production of Th1 and Th2 cytokines was observed at varying levels, even in cultures without exogenously added polarizing cytokines (Figures 1 and 2). We next analyzed in more detail the mechanism through which Ezh2 controls cytokine production in nonpolarized Th cell cultures with neutralizing antibodies to both IL-4 and IFN-γ. WT nonpolarized Th cells did not produce appreciable levels of Th1 or Th2 cytokines, but a substantial percentage of Ezh2-deficient cells produced IFN-γ (42.1%) and smaller percentages produced IL-4 and IL-13 (3.4% and 17.3%, respectively) (Figure 5A). These data confirm that loss of Ezh2 results in deregulation of both Th1 and to a lesser extent Th2 effector cell subtypes in the absence of exogenous polarizing signals. In nonpolarized Ezh2-deficient Th cells, *Tbx21* mRNA was increased 11.3-fold, there was a large 49.5-fold increase in the expression of the related T-box transcription factor gene *Eomes*, and there was a more modest 3.1-fold increase in *Gata3* expression (Figure 5B). Corresponding increases in expression of T-bet, Eomes, and Gata3 proteins were also detected by intracellular staining and flow cytometry (Figure 5C).

To determine the relative contribution of Ezh2-mediated repression of *Tbx21* and *Eomes* to the deregulated IFN-γ expression by Ezh2 KO cells, we next compared Th cells doubly deficient in Ezh2 and T-bet with Th cells doubly deficient in Ezh2 and Eomes (*Ezh2*$^{\Delta SET/\Delta SET}$*Eomes*$^{\Delta Exon1/\Delta Exon1}$). Interestingly, cells doubly deficient in Ezh2 and T-bet produced only moderately less IFN-γ under nonpolarized conditions compared to Ezh2-deficient cells (Figures 5D and S5A), indicating that T-bet plays only a minor role in the spontaneous production of IFN-γ by Ezh2-deficient Th cells. In contrast, in cultures with exogenously added IL-12, the enhancement of IFN-γ production induced by loss of Ezh2 was more dependent on T-bet (Figures 2E and S5A). We next analyzed the contribution of Eomes to the enhanced production of IFN-γ by both nonpolarized and Th1 polarized Ezh2-deficient cells. Nonpolarized Ezh2-deficient Th cells again produced IFN-γ, but strikingly, the spontaneous production of IFN-γ was completely lost in Th cells doubly deficient in Ezh2 and Eomes (Figures 5E, top, and S5A), indicating that Ezh2-mediated repression of *Eomes* is essential to avoid spontaneous production of IFN-γ. In contrast, Ezh2 and Eomes double deficiency had only a mild effect on the production of IFN-γ induced by IL-12 (Figures 5E, bottom, and S5A). Therefore, Ezh2-mediated repression of both T-bet and Eomes is required to efficiently control IFN-γ production by activated Th cells. Ezh2 appears to modulate the sensitivity of Th cells to IL-12 via control of the *Tbx21* locus, and Ezh2 is also required to repress the *Eomes* locus to avoid spontaneous expression of IFN-γ.

In nonpolarized Th cells, we detected large amounts of H3K27me3 at the *Eomes* locus, and this modification was lost in the absence of Ezh2 (Figure 5F). As expected, the presence of Ezh2 at the *Eomes* locus was not detected in *Ezh2*$^{\Delta SET/\Delta SET}$ Th cells (Figure 5G). To further investigate possible mechanisms regulating the upregulation of *Eomes* in Ezh2-deficient Th cells, we next measured histone acetylation (ac), an epigenetic modification associated with accessible chromatin structure and active transcription. We found that both H3K9ac (Figure 5H) and H3K27ac (Figure 5I) were increased at the *Eomes* locus in cells lacking Ezh2. Both p300 and CBP contain a histone acetyltransferase (HAT) domain and form a coactivation complex that can recruit RNA polymerase and enhance gene expression. We found higher binding of both of these proteins to the *Eomes* locus in Ezh2-deficient cells (Figures 5J and 5K). We also detected modestly enhanced histone acetylation and accumulation of p300 and CBP at the *Tbx21* locus in Ezh2-deficient cells compared to WT cells (Figures S5B–S5E). It is therefore likely that the p300/CBP HAT complex plays a role in the spontaneous enhancement of *Eomes* and possibly *Tbx21* expression in the absence of Ezh2 function.

Ezh2-Deficient Th Cells Display Enhanced Plasticity

We next investigated whether Ezh2 was also involved in regulating the maintenance of CD4+ T cell phenotype after specialization into effector Th1 or Th2 cells. WT and Ezh2-deficient CD4+ T cells were differentiated into Th1 or Th2 cells for 3 days (primary culture) and then cells were cultured under the opposite conditions for a further 2 days (secondary culture) and assessed for their ability to produce effector cytokines. Very little production of IL-4 or IL-5 was detected in WT or Ezh2-deficient primary Th1 cell cultures, but Ezh2-deficient cells could still produce some IL-13 (Figure 6A). In contrast, when polarized Th1 cells were exposed to Th2 cell-inducing secondary culture, we observed much stronger induction of IL-4, IL-5, and IL-13 in Ezh2-deficient cells compared to WT cells (4.8, 7.6, and 8.8 times, respectively) (Figure 6A). In addition, compared to WT cells, we detected increased IFN-γ production by Th2 polarized Ezh2-deficient cells, and this was further enhanced in response to secondary culture under Th1 cell-inducing conditions (2.8 times) (Figure 6B). We next stained WT and Ezh2-deficient Th2 cells with both IFN-γ and IL-4. Polarized Ezh2-deficient Th1 cells could be readily induced to express IL-4, IL-5, and IL-13 when exposed to Th2 cell-inducing culture conditions (Figure 6C). Importantly, we detected both single- and double-positive populations in cells lacking Ezh2, indicating that IFN-γ-producing Th1 cells were induced to express IL-4 in the absence of Ezh2 function. Similar plasticity in cytokine production was observed in Ezh2-deficient Th2 cells; when exposed to Th1 cell-inducing conditions, Ezh2-deficient Th2 cells expressed IFN-γ and a large percentage of these cells produced both IFN-γ and IL-4 (Figure 6D). In contrast to the instability observed in both Th1 and Th2 cell differentiation programs, stable repression of Th17 cell differentiation by Th1 cells was not affected by loss of Ezh2 (Figure S6A).

WT and Ezh2-deficient Th1 cells expressed similar levels of Gata3; however, after exposure to Th2 cell-inducing conditions,

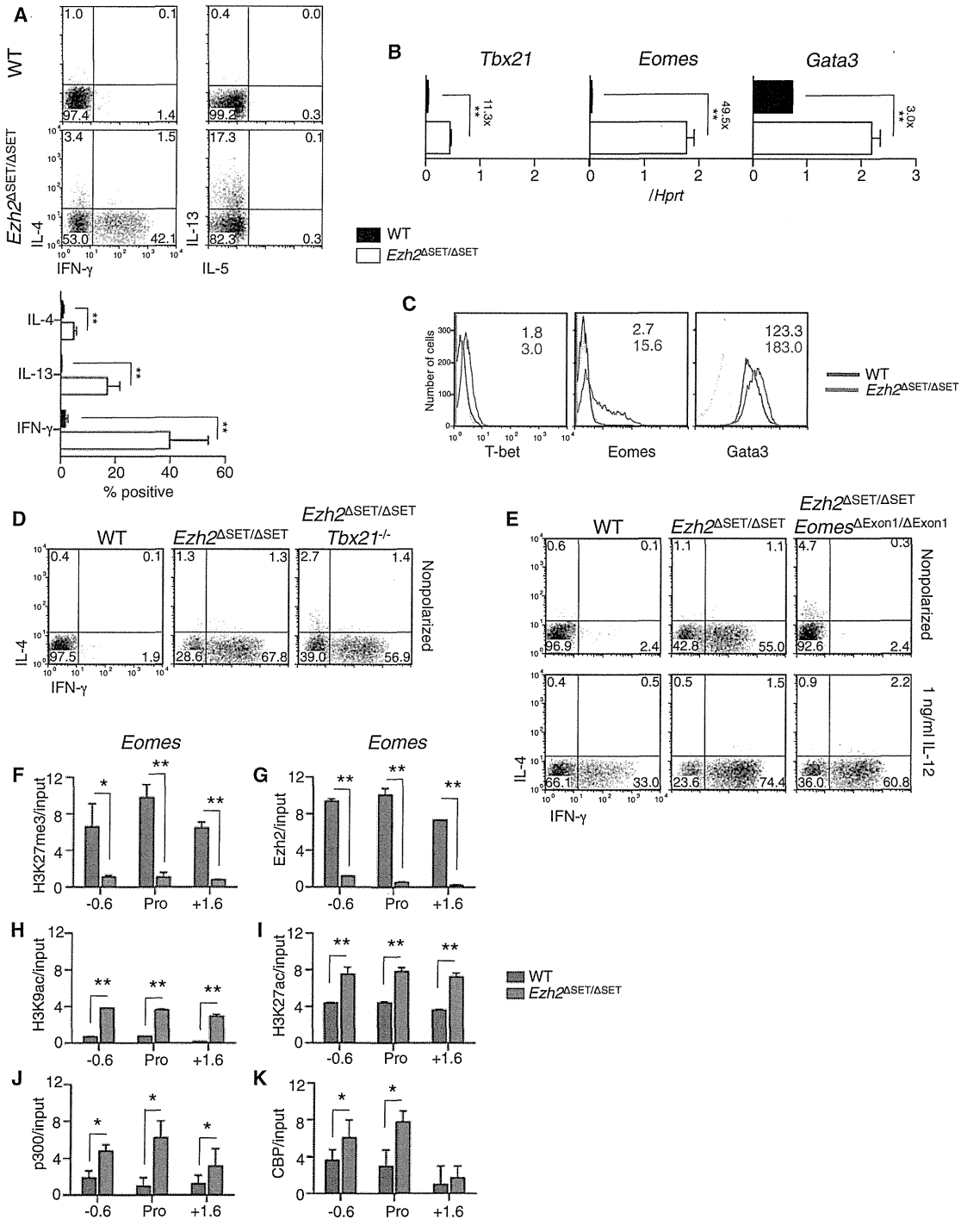

Figure 5. Ezh2-Mediated Repression of T-bet and Eomes Is Required to Control IFN-γ Production by Th Cells

(A–C) Naive WT and *Ezh2*$^{\Delta SET/\Delta SET}$ CD4$^+$ T cells differentiated under nonpolarizing conditions (with both anti-IL-4 and anti-IFN-γ neutralizing antibodies) followed by cytoplasmic staining of the indicated cytokines after 5 hr restimulation with anti-TCRβ (A, top) and combined results from five independent experiments (A, bottom), mRNA encoding *Tbx21*, *Eomes*, and *Gata3* (B), and protein expression of T-bet, Eomes, and Gata3 with MFIs shown (WT, blue; *Ezh2*$^{\Delta SET/\Delta SET}$, red) and 9,000 events displayed for each sample (C).

(D and E) Naive WT, *Ezh2*$^{\Delta SET/\Delta SET}$, and *Ezh2*$^{\Delta SET/\Delta SET}$*Tbx21*$^{-/-}$ double-deficient (D) or naive WT, *Ezh2*$^{\Delta SET/\Delta SET}$, and *Ezh2*$^{\Delta SET/\Delta SET}$*Eomes*$^{\Delta Exon1/\Delta Exon1}$ double-deficient (E) CD4$^+$ T cells differentiated under nonpolarizing (top) or Th1 cell-inducing conditions with 1 ng/ml IL-12 (bottom), and cytokine production measured by cytoplasmic staining of IL-4 and IFN-γ after 5 hr restimulation with anti-TCRβ.

(F–K) ChIP analysis for the indicated histone modifications and chromatin-modifying proteins at the *Eomes* locus in WT and *Ezh2*$^{\Delta SET/\Delta SET}$ nonpolarized Th cells. n = 3, mean ± SD. Data are representative of at least three independent experiments, *p < 0.05. **p < 0.01. See also Figure S5.

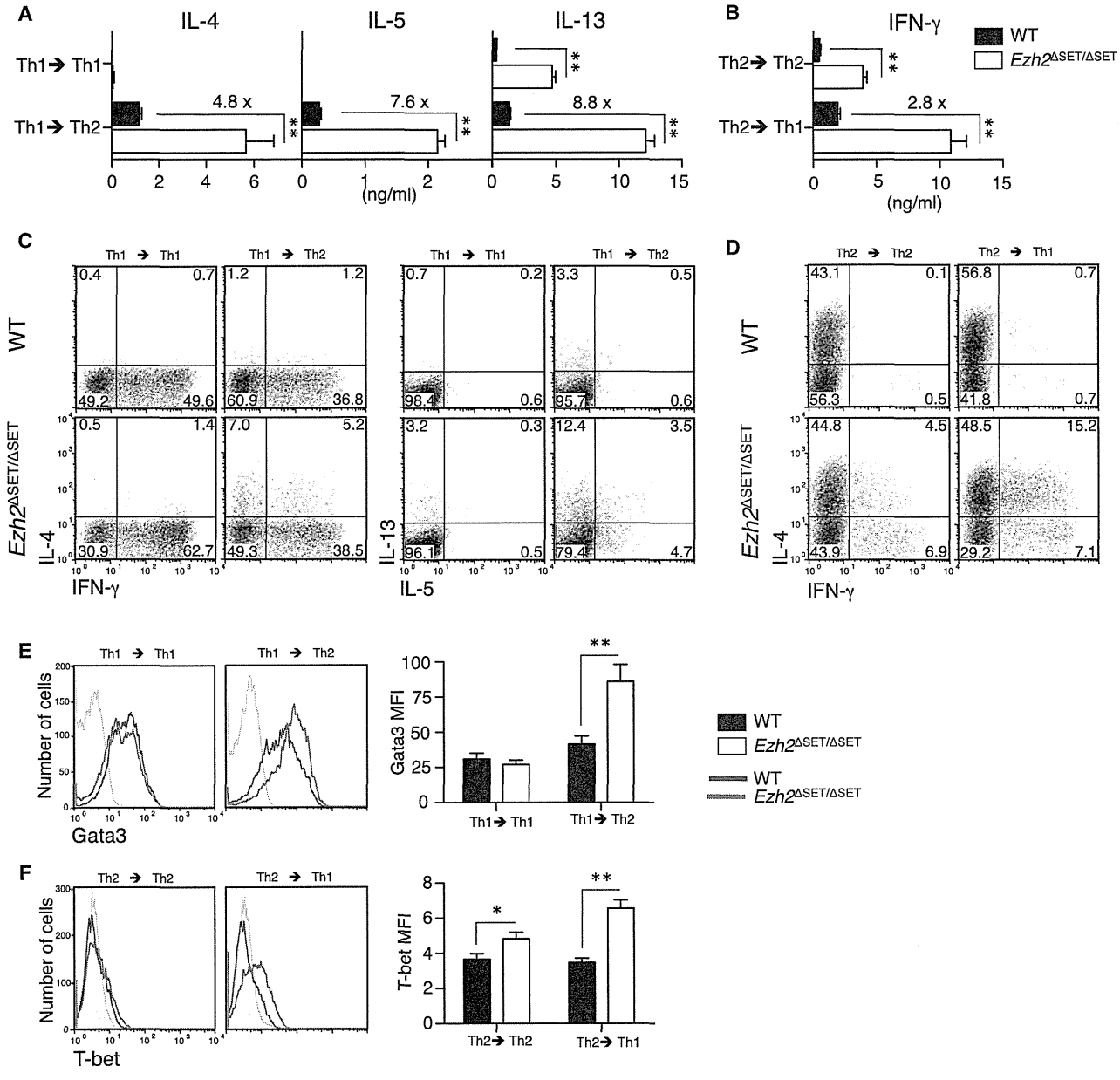

Figure 6. Loss of Ezh2 Results in Enhanced Plasticity of Th1 and Th2 Cells

Naive CD4+ T cells were polarized for 3 days under Th1 (A, C, and E) or Th2 (B, D, and F) cell-inducing conditions with 10 or 100 ng/ml of IL-12 or IL-4, respectively, and then recultured under the same condition or under the opposing condition for a further 2 days as indicated.

(A and B) Production of IL-4, IL-5, and IL-13 (A) and IFN-γ (B) measured by ELISA after 24 hr restimulation with anti-TCRβ, n = 3, mean ± SD.

(C–F) Cytoplasmic staining for IFN-γ with IL-4 (C and D) or IL-5 with IL-13 (C) and Gata3 alone (E), or T-bet alone (F) after 5 hr restimulation with anti-TCRβ.

(E and F) Histograms at left with 9,000 events displayed for each sample (WT, blue; *Ezh2*$^{\Delta SET/\Delta SET}$, red), and right panels show combined MFI results from five independent experiments.

All other data are representative of at least three independent experiments. **p < 0.01. See also Figure S6.

we observed a large increase in Gata3 expression in Ezh2-deficient Th1 cells (Figures 6E). Expression of T-bet was also higher in Ezh2-deficient compared to WT Th2 cells, and this was further enhanced by exposure to Th1 cell-inducing conditions (Figures 6F). Eomes was not expressed by Th2 cells after exposure to Th1 cell-inducing conditions (data not shown). Double staining of Gata3 with IL-4 showed a large increase in the number of Ezh2-deficient cells coexpressing Gata3 and IL-4 after Th2 cell-inducing secondary culture (Figure S6B). Ezh2 deficiency also enhanced the numbers of Th2 cells that coexpressed IFN-γ and T-bet after Th1 cell-inducing secondary culture (Figure S6C). These results show that both Th1 and Th2 cells lacking Ezh2 display considerably greater plasticity when compared to cells with intact Ezh2 function.

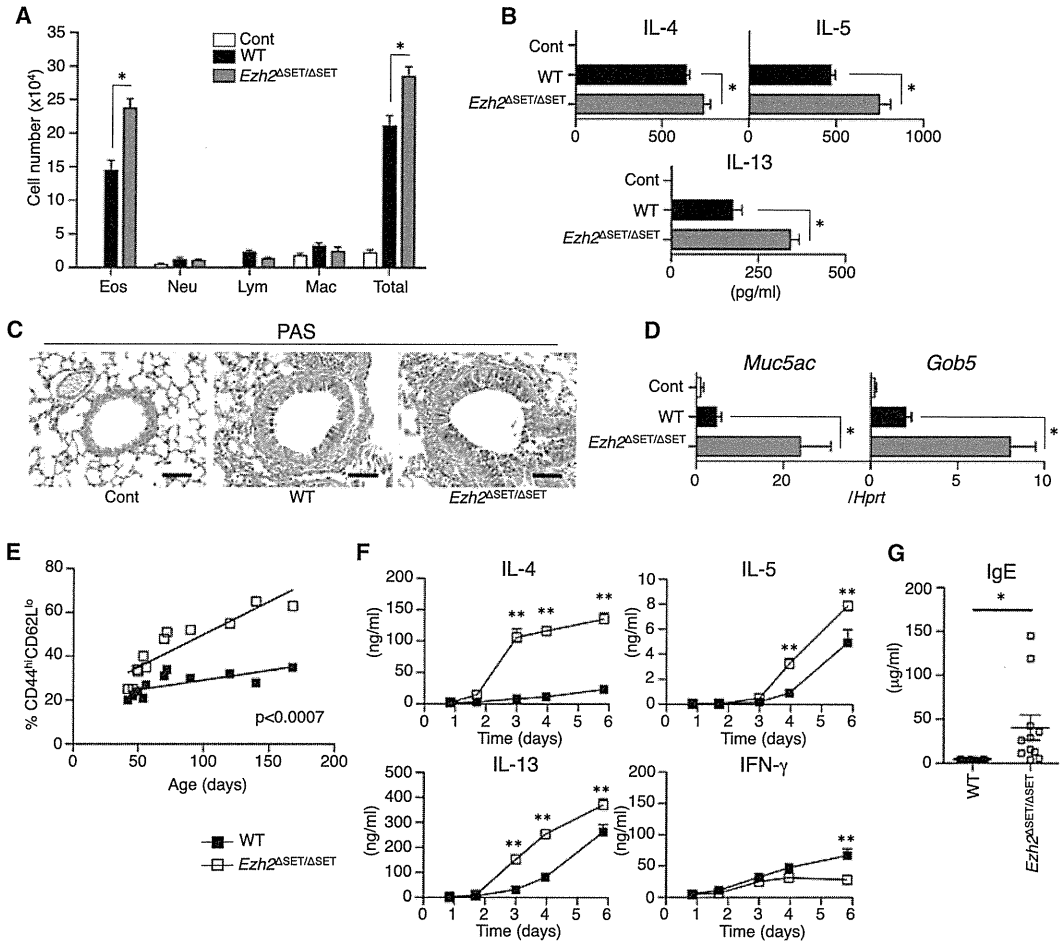

Figure 7. Th Cells Lacking Ezh2 Mediate Enhanced Type 2 Immune Responses In Vivo

(A–D) OVA-specific WT or *Ezh2*$^{\Delta SET/\Delta SET}$ Th2 cells were transferred to syngeneic WT C57BL/6 mice that were then challenged with an OVA aerosol. Total numbers of eosinophils (Eos), neutrophils (Neu), lymphocytes (Lym), and macrophages (Mac) recovered by bronchoalveolar lavage (BAL) (A) and indicated cytokines in cell-free BAL samples measured by ELISA (B). Representative images from lung tissue sections stained with periodic acid Schiff's reagent with mucus stained magenta; scale bars represent 60 μm (C). *Muc5ac* and *Gob5* mRNA expression in lung tissue measured by qRT-PCR (D).

(E–G) Untreated WT or *Ezh2*$^{\Delta SET/\Delta SET}$ mice analyzed for CD44^{hi}CD62L^{lo} spleen CD4$^+$ T cells by flow cytometry (E), and cytokine production by CD44^{hi}CD62L^{lo} spleen CD4$^+$ T cells stimulated with anti-TCRβ for the indicated times (F) and total serum IgE (G) measured by ELISA.

n = 5–6 mice/group (A–D); n = 11 mice/group (G); and n = 3 replicates (F) (all mean ± SEM). Data are representative of at least two independent experiments. *p < 0.05, **p < 0.01. In (E), p value determined by analysis of covariance. See also Figure S7.

Loss of Ezh2 Results in Enhanced Asthma-like Pathology and Accumulation of Th2 Memory Phenotype Cells In Vivo

Finally, to investigate the physiological consequences of Ezh2-mediated regulation of Th cell function, in vitro generated ovalbumin (OVA)-specific Th2 cells (Figure S7A) were intravenously transferred into WT C57BL/6 mice, and these mice were then challenged with aerosolized OVA. Compared to mice that received WT cells, recipients of Ezh2-deficient cells displayed increased eosinophilic inflammation in the airways, as assessed by bronchoalveolar lavage (BAL) (Figure 7A). In addition, mice that received Ezh2-deficient cells had higher levels of the Th2 cytokines IL-4, IL-5, and IL-13 in BAL samples (Figure 7B), and these mice displayed enhanced pathology and mucus hyperproduction in the lungs and higher expression of mRNA for *Muc5ac* and *Clca3* (*Gob5*) (Figures 7C and 7D).

In untreated mice maintained under specific-pathogen-free (SPF) conditions, we observed a progressive increase in the proportion of effector memory phenotype (CD44^{hi}CD62L^{lo}) CD4$^+$ T cells that was greatly exaggerated in mice with CD4$^+$ T cell-specific Ezh2 deficiency and accounted for approximately 70% of the CD4$^+$ T cells in the spleens of these mice by 6 months of age (Figure 7E). Interestingly, purified Ezh2-deficient effector memory phenotype CD4$^+$ T cells from 12-week-old mice produced markedly increased amounts of the Th2 cytokines IL-4, IL-5, and IL-13 but not IFN-γ when compared to WT effector memory phenotype cells (Figures 7F and S7B). Large increases in IgE were also detected in serum from 6-month-old mice with CD4$^+$ T cell-specific Ezh2 deficiency (Figure 7G). Thus, Th2 cells lacking Ezh2 generate exaggerated type 2 biased immune responses in a mouse model of allergic asthma, and loss of Ezh2 function in CD4$^+$

T cells results in enhanced accumulation of memory type Th2 cells in vivo.

DISCUSSION

The ability of CD4+ T cells to rapidly specialize into distinct subsets with defined functions is a critical aspect of immunoregulation. We have identified the polycomb protein Ezh2 as an essential regulator of Th1 and Th2 cell responses, both during differentiation and as a stabilizer of Th cell phenotype after specialization. Ezh2 directly bound and regulated correct expression of *Tbx21* and *Gata3* in developing Th1 and Th2 cells, and Ezh2 binding at these loci was accompanied by substantial H3K27me3. Ezh2 also constrained spontaneous generation of IFN-γ-producing cells, mainly by repressing expression of *Eomes*. In vivo, loss of Ezh2 enhanced Th2 cell-induced pathology in a model of allergic asthma and in untreated animals resulted in progressive accumulation of memory phenotype Th2 cells.

Ezh2 bound strongly to *Tbx21* and *Gata3*, and these two master regulators displayed the highest levels of differential binding between Th1 and Th2 cells. In addition, we detected strong binding of Ezh2 to the gene *Eomes* that encodes another T-box transcription factor closely related to T-bet. Inactivation of Ezh2 resulted in a profound reduction in H3K27me3, confirming that in CD4+ T cells functional Ezh2 is required for maintenance of H3K27me3 at each of these loci. However, it should be noted that although Ezh2 occupancy at genes encoding the Th1 and Th2 cytokines was at the lower limits of detection in both ChIP-PCR and ChIP-seq assays, we could still detect H3K27me3 at these loci that was lost in cells deficient in Ezh2. This may indicate that very low levels of Ezh2 binding could still have some control over H3K27me3 at these loci. Based on the results obtained with Th cells doubly deficient in Ezh2 together with T-bet or Ezh2 together with Eomes, Ezh2-mediated regulation of sensitivity to IL-12-induced Th1 cell polarization and spontaneous generation of IFN-γ-producing cells can be largely explained by the repression of *Tbx21* and *Eomes* expression. However, Th1 cells lacking T-bet could still produce appreciable amounts of IFN-γ, a result that has also been shown previously (Usui et al., 2006) and attributed to a decreased requirement for T-bet when IL-4 signals are neutralized. Likewise, Th cells doubly deficient in Ezh2 and T-bet could still produce significant amounts of IFN-γ, indicating that Ezh2 could also be involved in the regulation of other IFN-γ-inducing genes or the *Ifng* locus itself. It is also possible that Ezh2-mediated repression of *Gata3* together with repression of other loci such as the Th2 cytokine genes may contribute to the control of Th2 cell polarization. We also detected enhanced expression of c-Maf (encoded by *Maf*) in Ezh2-deficient Th cells. However, *Maf* does not appear to be a direct target of Ezh2, and no difference in Ezh2 binding at this locus was detected in Th1 compared to Th2 cells, indicating that *Maf* may be indirectly regulated in cells lacking Ezh2 function.

During differentiation of Ezh2-deficient Th cells, *Tbx21* and *Gata3* were more sensitive to upregulation in response to polarizing cytokines. This phenotype contrasts with that observed for T cells lacking DNA methyltransferase (*Dnmt1*), where dysregulated expression of IL-4 appears to be independent of Gata3 expression (Makar et al., 2003). Moreover, repression of cytokine production by Dnmt3a appears to depend on de novo methylation at the *Il4*, *Il13*, and *Ifng* loci (Thomas et al., 2012; Yu et al., 2012). In contrast, our data show that Ezh2-deficient cells maintain the ability to polarize into Th1 or Th2 cell subsets, accompanied by upregulation of the corresponding master regulator. Therefore, histone methyltransferases and DNA methyltransferases appear to control Th cell function through the regulation of distinct target genes. Interestingly, it was recently found that the SUV39H1-H3K9me3-HP1α pathway is also required to maintain Th2 cell stability and that loss of SUV39H1 changes the ratio of H3K9ac to H3K9me3 at the *Ifng* locus (Allan et al., 2012). In addition to directly binding to *Tbx21, Eomes*, and *Gata3*, we found that Ezh2 inhibited spontaneous accumulation of the HAT coactivator proteins p300 and CBP and of H3K9ac and H3K27ac at the *Tbx21* and *Eomes* loci.

Ezh2 does not appear to play a major role in the repression of other Th cell differentiation programs. Th17 cell polarization and stable repression of Th17 cell differentiation are less sensitive to loss of Ezh2, and Th9 cell and iTreg cell differentiation is actually inhibited in the absence of Ezh2. Impaired differentiation of Ezh2-deficient Th9 and iTreg cells may be due to the inability of these cells to repress IFN-γ, leaving open the possibility that Ezh2 may have important as yet undiscovered effects on differentiation of these cell types. In contrast to *Tbx21*, *Eomes*, and *Gata3*, Ezh2 does not appear to target the master regulators of other lineages, specifically *Rorc* (Th17 cells), *Foxp3* (iTreg cells), or *Sfpi1* or *Irf4* (Th9 cells). Eomes may control IFN-γ expression by CD4+ T cells under some circumstances (Suto et al., 2006; Tofukuji et al., 2012; Yang et al., 2008), but Eomes is not highly expressed in IL-12-induced Th1 cells. Our data indicate that Ezh2-mediated repression of *Eomes* is essential to inhibit spontaneous expression of IFN-γ production when not directly inhibited by other Th cell differentiation programs. It will therefore be important to further investigate the functional role for Ezh2-mediated repression of *Eomes* in other Th cell subsets.

We also found that Ezh2-deficient Th cells were capable of causing enhanced airway inflammation and pathology and that loss of Ezh2 function in CD4+ T cells resulted in progressive accumulation of Th2 cytokine-producing cells with a memory phenotype over the life of the animal, accompanied by strong increases in circulating IgE. Several other lines of mice with mutations in genes encoding signaling molecules in T cells have previously been reported to display similar increases in CD44hi cells with a Th2 cell phenotype and increases in type 2 inflammation in vivo. However, in these cases, severe alterations in thymic development (Aguado et al., 2002; Ji et al., 2007) or lymphocyte proliferation (Ranger et al., 1998) are evident. Although the exact mechanisms underlying the progressive Th2 cell-biased phenotype of SPF-maintained mice with CD4+ cell-specific deletion of Ezh2 remain unclear, it will be important to further explore the function of Ezh2 in other Th cell lineages, for example iTreg cells, as well as at other Ezh2 target genes that may contribute to Th2 cell-mediated inflammation.

In summary, we found that Ezh2 binds strongly to the master regulators of Th1 and Th2 cell differentiation *Tbx21* and *Gata3*, respectively, and its presence is linked to the maintenance of the H3K27me3 mark at these loci. Ezh2 is essential for controlling differentiation, cytokine production, and maintenance of polarization of CD4+ Th cells. We also identified a pathway